The Astrophysical Journal, 630:250–268, 2005 September 1

A GENERAL THEORY OF TURBULENCE-REGULATED STAR FORMATION, FROM SPIRALS TO ULTRALUMINOUS INFRARED GALAXIES

Mark R. Krumholz
Physics Department, University of California, 366 LeConte Hall, Berkeley, CA 94720; krumholz@astron.berkeley.edu

and

Christopher F. McKee
Departments of Physics and Astronomy, University of California, 366 LeConte Hall, Berkeley, CA 94720; cmckee@astron.berkeley.edu
Received 2005 March 18; accepted 2005 May 9

ABSTRACT

We derive an analytic prediction for the star formation rate in environments ranging from normal galactic disks to starbursts and ULIRGs in terms of the observables of those systems. Our calculation is based on three premises: (1) star formation occurs in virialized molecular clouds that are supersonically turbulent; (2) the density distribution within these clouds is lognormal, as expected for supersonic isothermal turbulence; and (3) stars form in any subregion of a cloud that is so overdense that its gravitational potential energy exceeds the energy in turbulent motions. We show that a theory based on this model is consistent with simulations and with the observed star formation rate in the Milky Way. We use our theory to derive the Kennicutt-Schmidt law from first principles and make other predictions that can be tested by future observations. We also provide an algorithm for estimating the star formation rate that is suitable for inclusion in numerical simulations.

Subject headings: galaxies: ISM — hydrodynamics — ISM: clouds — ISM: kinematics and dynamics — stars: formation — turbulence

1. INTRODUCTION

The disk of the Milky Way contains $\sim 10^9\ M_\odot$ of molecular gas (Williams & McKee 1997; Bronfman et al. 2000), mostly arranged in giant molecular clouds (GMCs) with typical masses of $\sim 10^6\ M_\odot$ and densities $n_{\rm H} \sim 100\ {\rm cm}^{-3}$ (Solomon et al. 1987). Absent other support, this gas should collapse on its free-fall timescale, $t_{\rm ff} \sim 4$ Myr, producing new stars at a rate of roughly $\sim 250\ M_\odot\ {\rm yr}^{-1}$. However, the observed star formation rate (SFR) in the Milky Way is only $\sim 3\ M_\odot\ {\rm yr}^{-1}$ (McKee & Williams 1997). This surprisingly low SFR, first pointed out by Zuckerman & Evans (1974), remains one of the major unsolved riddles for theories of the interstellar medium (ISM).

In the last 30 years, observations of star formation tracers such as Hα in other galaxies have shown that the problem is not limited to the Milky Way. Wong & Blitz (2002) inferred gas depletion times, defined as the ratio of the molecular surface density to the SFR per unit area, of a few billion years in resolved observations of seven nearby galaxies. This is 2 orders of magnitude larger than the typical free-fall times of a few tens of millions of years they inferred based on the cloud densities. Rownd & Young (1999) and Young et al. (1996) obtain similar gas depletion times from unresolved observations in many other galaxies. Nor is the problem limited to normal disk galaxies like the Milky Way. In 87 starbursts Gao & Solomon (2004) find CO gas depletion times of several hundred million to several billion years, a factor of 10 or less smaller than that in disk galaxies, and still much longer than typical free-fall times. Downes & Solomon (1998) obtain relatively similar depletion times at comparable densities for circumnuclear starbursts in three nearby galaxies, and this range of depletion times and characteristic free-fall times seems typical of starbursts (Kennicutt 1998b).

An interesting addition to this problem is that the SFR follows clear correlations. Surveys of many galaxies over a range of SFRs and surface densities show that the SFR per unit area obeys the Kennicutt-Schmidt law, which can be stated in two forms, both equally consistent with observations:

$$\dot{\Sigma}_* \propto \Sigma_g^{1.4} \tag{1}$$

or

$$\dot{\Sigma}_* \propto \frac{\Sigma_g}{\tau_{\rm dyn}}, \tag{2}$$

where $\dot{\Sigma}_*$ is the SFR per unit area, Σ_g is the surface density of gas, and $\tau_{\rm dyn}$ is the dynamical (i.e., orbital) timescale of the galactic disk (Schmidt 1959, 1963; Kennicutt 1998a, 1998b; Schmidt's two papers proposed a relationship between gas density or surface density and SFR, while Kennicutt's determined the exponents and coefficients of the correlations in eqs. [1] and [2] from a large galaxy sample). Both forms fit the observed sample of galaxies very well over a range of nearly 8 orders of magnitude in SFR.

Any successful theory of star formation must be able to reproduce both the lower than expected SFR and both forms of the Kennicutt-Schmidt law and must do so using physics that is applicable in a range of environments from Milky Way–like disk galaxies, where the ISM is entirely atomic and the SFR is low, to ultraluminous infrared galaxies (ULIRGs), where the ISM is fully molecular and the SFR is many orders of magnitude larger. To date, no theory is able to meet these requirements. Recent numerical work has been able to reproduce some of the observations, but only with considerable assumptions and limitations. Kravtsov (2003) uses the probability distribution of densities in simulations to suggest that the fraction of high-density gas varies with the overall density to roughly the 1.4 power, explaining one form

of the Kennicutt-Schmidt law. However, this observation does not explain the other form of the law, and it also says nothing about the absolute rate at which star formation occurs. It also fails to explain the choice of density cutoff that constitutes "high density." Similarly, Li et al. (2005) show that their simulations reproduce the $\Sigma_g^{1.4}$ form of the Kennicutt-Schmidt law. However, their simulations depend on both an arbitrarily chosen density threshold for star formation and an arbitrary choice of the SFR in gas denser than the threshold.

Tan (2000) proposes an analytic theory based on star formation induced by cloud-cloud collisions to explain the Kennicutt-Schmidt law. In this model, the SFR is proportional to $\Sigma_g/\tau_{\rm dyn}$ because the intercloud collision time is proportional to the dynamical time, and the supply of gas available is proportional to the gas surface density. However, this theory also relies on an unknown efficiency of (collision induced) star formation that can be roughly calibrated from observations but is not independently predicted. Similarly, Silk (1997) proposes a theory in which the SFR is set by supernova feedback. However, the theory depends critically on the porosity P of the ISM to gas heated by supernovae, and it is unclear how P varies from the predominantly atomic, diffuse gas disks found in normal galaxies like the Milky Way to the dense, entirely molecular interstellar media found in starbursts. In particular, the theory predicts that if P is roughly constant (as is required to obtain the observed SFR and the Kennicutt-Schmidt law), then all galaxies should have the same ISM velocity dispersion. This prediction clearly fails in starbursts (Downes & Solomon 1998).

Another broad class of theories appeals to magnetic fields and ambipolar diffusion. In these models, star-forming regions are threaded by a magnetic field strong enough to make them magnetically subcritical, so the collapse time is set by the time required for the field to escape from the gas via ambipolar diffusion (see reviews by Shu et al. 1987; Mouschovias 1987; for a more recent discussion see Tassis & Mouschovias 2004). While we discuss this theory in more detail in § 7.3, we note that observations of magnetic field strengths in Milky Way GMCs, both directly via Zeeman splitting (Crutcher 1999; Bourke et al. 2001) and indirectly via statistical indicators (Padoan et al. 2004), suggest that their magnetic fields are not strong enough by themselves to prevent rapid collapse. Nothing is known of magnetic field strengths in other galaxies, so it is unknown if this model can explain the Kennicutt-Schmidt law.

A final class of theories, on which we focus here, relies on turbulence. Observed GMCs in the Milky Way and in nearby galaxies have significant nonthermal line widths (e.g., Fukui et al. 2001; Engargiola et al. 2003; Rosolowsky & Blitz 2005), and this is generally interpreted as indicating the presence of supersonic turbulence. In a cloud supported against collapse by supersonic turbulence, at any given time most of the mass should be in structures that are insufficiently dense to collapse (see reviews by Mac Low & Klessen 2004; Elmegreen & Scalo 2004). This conclusion is bolstered by simulations (e.g., Klessen et al. 2000; Li et al. 2004) that show that, under at least some circumstances, supersonic turbulence can inhibit star formation.

Padoan (1995) provides an analytic theory of the SFR in a turbulent medium that depends on the properties of GMCs and on the distribution of masses of clumps that results from turbulent fragmentation. For Milky Way GMCs it produces a value of the SFR reasonably in agreement with observations, but there is no way to extend this result to galaxies where we cannot directly observe the GMCs. Similarly, Elmegreen (2002, 2003) uses the probability distribution function (PDF) of densities in a turbulent medium to estimate the mass fraction of Galactic GMCs above a critical density of $\sim 10^5$ cm^{-3} and argues that this can explain the low SFR. However, it is not clear why the critical density is 10^5 cm^{-3} or how this value might vary from galaxy to galaxy. Nor is it clear how this analysis leads to the Kennicutt-Schmidt law. Elmegreen argues that the law $\dot{\Sigma}_* \propto \Sigma_g^{1.4}$ can be explained in this picture if all galaxies have roughly the same scale height but does not provide a physical reason why the scale height should be constant.

Our goal in this paper is to provide a theory of the SFR that can explain both the surprisingly low SFR and two forms of the Kennicutt-Schmidt law and that can do so over a range of conditions from normal disks to ULIRGs. In other words, we seek to explain both the exponents and the coefficients of the Kennicutt-Schmidt laws over their entire observed range. Our theory does not depend on an unknown efficiency or critical density for star formation. Instead, we proceed from three premises that are well motivated by a combination of observations, simulations, and theoretical considerations. First, we assume that star formation occurs primarily in molecular clouds that are virialized and supersonically turbulent. Second, we assume that the probability distribution of densities is lognormal, as expected for supersonic isothermal turbulence. Third, we assume that gas collapses in regions where the local gravitational potential energy exceeds the local turbulent energy. In § 2 we develop these premises to compute the SFR in a cloud in terms of its Mach number and virial parameter. We check this theory against simulations and show that it is able to reproduce them well. In § 3 we apply our estimate to galaxies and derive an estimate for the SFR as a function of the observable properties of galaxies. In § 4 we compare our theoretical predictions to the observed SFRs in the Milky Way, and in § 5 we compare to a large sample of galactic-average SFRs. We show that our theory provides an excellent fit to the data. In § 6 we present three future observations that can be used to check our theory. Finally, in §§ 7 and 8 we discuss and summarize our conclusions.

2. THE STAR FORMATION RATE PER FREE-FALL TIME

In this section we present our general theory of turbulent regulation of the SFR in dimensionless terms. For convenience we define the dimensionless SFR per free-fall time, $\mathrm{SFR}_{\rm ff}$, which is the fraction of an object's gaseous mass that is transformed into stars in one free-fall time at the object's mean density.

2.1. *Derivation*

Both simulations and observations of turbulence in the ISM show that the turbulent velocity dispersion σ_l computed over a volume of characteristic length l increases with l as $\sigma_l \propto l^p$ with $p \approx 0.5$ (Larson 1981; Solomon et al. 1987; Heyer & Brunt 2004). This self-similar structure appears to be a universal property of supersonic turbulence and holds over a very wide range of length scales in molecular clouds. Ossenkopf & Mac Low (2002) summarize observations of the Polaris flare molecular cloud that show the line width–size relation over 3 orders of magnitude in length. Because velocity dispersions are smaller on smaller scales, even though the velocity dispersion may be supersonic over length scales comparable to the size of a simulation box or an entire star-forming cloud, there will be some smaller scale over which it is not. Vázquez-Semadeni et al. (2003, hereafter VBK03) show that the scale at which the turbulence transitions from supersonic to subsonic, the sonic length λ_s, is a key determinant of whether $\mathrm{SFR}_{\rm ff}$ will be high or low. For the purposes of this paper, we adopt a more specific definition of the sonic length, consistent with that of VBK03: let $\sigma_l(\boldsymbol{x})$ be the one-dimensional velocity

dispersion computed over a sphere of diameter l centered at position $\boldsymbol{x}$ within a turbulent medium, and let

$$\sigma_l = \langle \sigma_l(\boldsymbol{x}) \rangle_V \tag{3}$$

be the volume average of $\sigma_l(\boldsymbol{x})$ over the entire region. We define λ_s as the length l such that $\sigma_l = c_s$, where c_s is the isothermal sound speed in the region (note that our λ_s is the same as the turbulent pressure length l_P introduced by Wolfire et al. 2003). The line width–size relation then becomes

$$\sigma_l = c_s \left(\frac{l}{\lambda_s} \right)^p. \tag{4}$$

While VBK03 show that the sonic length correlates well with $\mathrm{SFR_{ff}}$, the SFR per free-fall time is a dimensionless number and the sonic length is a length. On dimensional grounds, there must therefore be another length scale that is relevant. The natural candidate is the Jeans length,

$$\lambda_{\mathrm{J}} = \sqrt{\frac{\pi c_s^2}{G\rho}}, \tag{5}$$

where c_s is the sound speed and ρ is the density at a given point. Of course, in a turbulent medium ρ varies from place to place, and we account for this effect below. Consider a "core," a sphere of gas embedded in the cloud. The thermal pressure at the surface of the sphere is roughly ρc_s^2. The largest mass such an object can have and remain stable against gravitational collapse is the Bonnor-Ebert mass (Ebert 1955; Bonnor 1956),

$$M_{\mathrm{BE}} = 1.18 \frac{c_s^3}{\sqrt{G^3 \rho}} \tag{6}$$

$$= \frac{1.18}{\pi^{3/2}} \rho \lambda_{\mathrm{J}}^3. \tag{7}$$

The radius of such a sphere is roughly

$$R_{\mathrm{BE}} \approx 0.37 \lambda_{\mathrm{J}}. \tag{8}$$

The gravitational potential energy of the sphere is

$$\mathcal{W} = -\frac{3}{5} a \frac{G M_{\mathrm{BE}}^2}{R_{\mathrm{BE}}} = -1.06 \frac{c_s^5}{G^{3/2} \rho^{1/2}}. \tag{9}$$

Here a is a geometric factor set by the sphere's mass distribution, and in the numerical evaluation we have used $a = 1.2208$, the value for a maximum-mass stable Bonnor-Ebert sphere (McKee & Holliman 1999). The thermal energy of the gas is

$$\mathcal{T}_{\mathrm{th}} = \frac{3}{2} M_{\mathrm{BE}} c_s^2 = 1.14 |\mathcal{W}|. \tag{10}$$

Using the line width–size relation given by equation (4), the average turbulent kinetic energy in the sphere is

$$\mathcal{T}_{\mathrm{turb}} = \frac{3}{2} M_{\mathrm{BE}} \sigma^2 (2R_{\mathrm{BE}}) \tag{11}$$

$$= 1.14 \ (0.74)^{2p} \left(\frac{\lambda_{\mathrm{J}}}{\lambda_s} \right)^{2p} |\mathcal{W}| \tag{12}$$

$$\rightarrow 0.89 \left(\frac{\lambda_{\mathrm{J}}}{\lambda_s} \right) |\mathcal{W}|, \tag{13}$$

where for the numerical evaluation in the final step we have used $p = 0.5$. Thus, a Bonnor-Ebert mass object has approximately equal kinetic, thermal, and potential energies if $\lambda_{\mathrm{J}} \sim \lambda_s$. If $\lambda_{\mathrm{J}} \lesssim \lambda_s$, gravity is approximately balanced by thermal plus turbulent pressure, and the object is at best marginally stable against collapse. If $\lambda_{\mathrm{J}} \gg \lambda_s$, kinetic energy greatly exceeds both potential and thermal energy, and the object is stable against collapse.

Since λ_{J} is a function of the local density, the condition $\lambda_{\mathrm{J}} \lesssim \lambda_s$ for collapse translates into a minimum local density required for collapse. We can use this to compute the SFR, by first estimating what fraction of the mass is at densities higher than this minimum. Numerous numerical and theoretical studies find that the PDF of the density in a supersonically turbulent isothermal gas is lognormal, with a dispersion that increases with Mach number (Vázquez-Semadeni 1994; Padoan et al. 1997; Scalo et al. 1998; Passot & Vázquez-Semadeni 1998; Nordlund & Padoan 1999; Ostriker et al. 1999; Padoan & Nordlund 2002). Padoan & Nordlund (2002) find that the PDF is well fitted by the functional form

$$dp(x) = \frac{1}{\sqrt{2\pi\sigma_\rho^2}} \exp\left[-\frac{\left(\ln x - \overline{\ln x} \right)^2}{2\sigma_\rho^2} \right] \frac{dx}{x}, \tag{14}$$

where $x = \rho/\rho_0$ is the density normalized to the mean density in the region ρ_0. The mean of the log of density is

$$\overline{\ln x} = -\frac{\sigma_\rho^2}{2}, \tag{15}$$

and the dispersion of the PDF is approximately

$$\sigma_\rho \approx \left[\ln\left(1 + \frac{3\mathcal{M}^2}{4} \right) \right]^{1/2}, \tag{16}$$

where $\mathcal{M}$ is the one-dimensional Mach number of the turbulent region measured on its largest scale. Let λ_{J0} be the Jeans length at the mean density. The Jeans length at overdensity x is $\lambda_{\mathrm{J}}(x) = \lambda_{\mathrm{J0}}/\sqrt{x}$, which we wish to compare with λ_s. We therefore define the critical overdensity required for collapse as

$$x \geq x_{\mathrm{crit}} \equiv \left(\phi_x \frac{\lambda_{\mathrm{J0}}}{\lambda_s} \right)^2, \tag{17}$$

where ϕ_x is a numerical factor to be determined by fitting in § 2.2. Gas at an overdensity of x_{crit} or higher has a local Jeans length smaller than the sonic length and is therefore unstable to collapse. The fraction of the mass in collapsing structures is therefore just the fraction of mass at overdensities of x_{crit} or greater, which is

$$f = \int_{x_{\mathrm{crit}}}^{\infty} x \frac{dp}{dx} \, dx. \tag{18}$$

To convert f to an SFR, we must account for two factors. First, approximately 25%–75% of the mass in star-forming cores will be ejected by outflows (Matzner & McKee 2000). We define ϵ_{core} as the fraction of the mass that reaches the collapsing core phase that eventually winds up in a star and adopt a fiducial value of $\epsilon_{\mathrm{core}} = 0.5$. Second, we have computed the fraction of mass in collapsing structures at any given time. To convert this to a rate, we must divide by the characteristic timescale over which new gas becomes unstable. When a region collapses, it detaches from the turbulent flow and thereby removes pressure support from

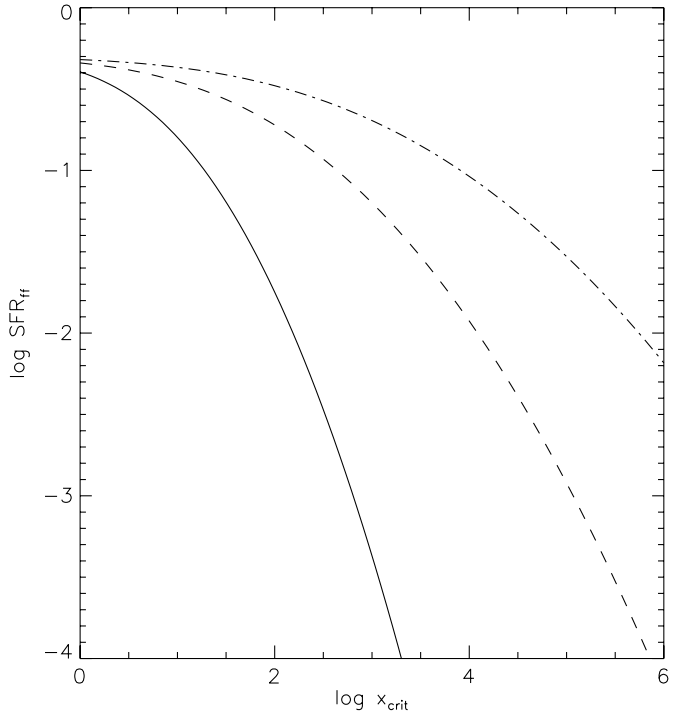

FIG. 1.—SFR per free-fall time vs. critical overdensity, for Mach numbers of 5 (*solid line*), 50 (*dashed line*), and 500 (*dot-dashed line*).

the remaining, stable gas. The remaining gas will respond to this loss of pressure support on its gravitational collapse timescale, the free-fall time. We therefore estimate that new gas becomes gravitationally unstable over a free-fall timescale $t_{\rm ff}$. (Alternately, we could have used a crossing time, which is very similar in a real GMC.) However, this is just a rough argument, so we let the true timescale be $\phi_t t_{\rm ff}$. We determine ϕ_t for purely hydrodynamic turbulence in § 2.2. Magnetic fields can delay collapse and make ϕ_t somewhat larger for a real cloud than our fit will find (Vázquez-Semadeni et al. 2005).

With these two factors defined, the SFR per free-fall time is

$$\mathrm{SFR}_{\rm ff} = \frac{\epsilon_{\rm core}}{\phi_t}\int_{x_{\rm crit}}^{\infty} xp(x)\,dx \tag{19}$$

$$= \frac{\epsilon_{\rm core}}{2\phi_t}\left[1+\mathrm{erf}\left(\frac{-2\ln x_{\rm crit}+\sigma_\rho^2}{2^{3/2}\sigma_\rho}\right)\right]. \tag{20}$$

The total SFR arising from a cloud of mass $M_{\rm mol}$ is

$$\dot{M}_* = \mathrm{SFR}_{\rm ff}\frac{M_{\rm mol}}{t_{\rm ff}}. \tag{21}$$

We plot $\mathrm{SFR}_{\rm ff}$ as a function of $x_{\rm crit}$ for $\phi_t = 1$ in Figure 1. We can also define a "core formation rate" $\mathrm{CFR}_{\rm ff}$, which reflects the rate at which mass begins to collapse, ignoring what fraction of it will be ejected by feedback. This is simply $\mathrm{SFR}_{\rm ff}$ with $\epsilon_{\rm core} = 1$.

Padoan (1995) and Padoan & Nordlund (2002, 2004) have previously approached the problem of estimating the SFR by considering the combination of the PDF of densities and the mass distribution of clumps created by fragmentation in a turbulent medium. Since we are interested only in the rate at which stars form, and not their mass distribution, we may neglect the clump mass distribution and consider only the distribution of densities. In so doing, we implicitly assume that all or most of the mass that is at densities rendering it capable of collapse will be in the presence of enough other high-density gas so that it does collapse. This assumption is bolstered by the observation that turbulence tends to organize mass into filaments and voids on large scales, so that high-density gas is likely to be in the presence of other high-density gas. Moreover, as we show in § 2.2, this assumption produces a theory that shows good agreement with simulations.

2.2. *Comparison to Simulations*

To test our theory, we compare to the work of VBK03, who simulated a turbulent periodic box of gas and computed the fraction of the mass that collapsed into stars. The simulation setup is described in detail in Klessen et al. (2000), but we summarize it here. In simulation units, the box length is $L = 2$, the sound speed is $c_s = 0.1$, the mean density is $\rho_0 = \frac{1}{8}$, the Jeans length at that density is $\lambda_{\rm J0} = \frac{1}{2}$, and the free-fall time is $t_{\rm ff} = 1.5$. Turbulence is driven at a one-dimensional Mach number $\mathcal{M} = 2$, 3.2, 6, or 10 using a driving field that contains power only at wavenumbers around $k = 2$, 4, or 8, where $k \equiv L/\lambda_d$ and λ_d is the driving wavelength.

We read off the sonic length from Figure 3*c* of VBK03, noting that VBK03 define the sonic length using the three-dimensional velocity dispersion, while we use the one-dimensional velocity dispersion (J. Ballesteros-Paredes and E. Vázquez-Semadeni 2005, private communication). Given the scaling $\sigma \propto l^p$ and assuming that the turbulent velocity field is roughly isotropic, the two are related by $\lambda_s \approx 3^{1/(2p)}\lambda_{s3}$. We adopt $p = 0.5$ through the rest of this section. To determine the $\mathrm{SFR}_{\rm ff}$, we read off data from Figure 2 of VBK03. We measure the time t at which a fraction $f = 0.1$ of the mass in the run has collapsed into stars. For runs where less than 10% of the mass has collapsed by the end, we measure f and t at the point where the run ends. We then compute $\mathrm{SFR}_{\rm ff} = 1.5f/t$. (Using 20% instead of 10% did not substantially change the result.) We summarize all of this in Table 1.

We fit the VBK03 data to our theoretical estimate of $\mathrm{CFR}_{\rm ff}$ rather than $\mathrm{SFR}_{\rm ff}$ because the VBK03 simulations do not include any feedback. The cases with large $x_{\rm crit}$ are closest to the environment in real star-forming clouds, so we weight by $x_{\rm crit}^2$. A Levenberg-Marquardt fit with this weighting gives $\phi_x = 1.12$ and $\phi_t = 1.91$. We compare the simulation to $\mathrm{CFR}_{\rm ff}$ evaluated

TABLE 1
MEASURED AND PREDICTED VALUES FROM VBK03 SIMULATIONS

Run Name (1)	λ_{s3} (2)	t (3)	$\mathrm{SFR}_{\rm ff,sim}$ (4)	$\mathrm{SFR}_{\rm ff,th}$ (5)
M2K2	0.16	0.62	0.24	0.33
M2K4	0.10	0.62	0.24	0.18
M2K8	0.20	0.62	0.24	0.39
M3.2K2	0.080	0.44	0.34	0.18
M3.2K4	0.046	1.58	0.095	0.0641
M3.2K8	0.031	2.48	0.060	0.023
M6K2	0.039	0.30	0.50	0.11
M6K4	0.023	2.27	0.066	0.045
M6K8	0.016	6.89	0.022	0.019
M10K2	0.018	0.87	0.17	0.060
M10K4[a]	0.013	6.03	0.014	0.035
M10K8[b]	0.0094	4.69	0.026	0.018

NOTES.—Col. (1): Run name in VBK03. M*m*K*k* indicates that the one-dimensional Mach number is *m* and the run is driven at wavenumber *k*. Col. (2): Measured value of λ_{s3}. Col. (3): Time at which 10% of the mass had collapsed, or when the run ended, in code units. Col. (4): Star formation rate in the simulation, defined as $\mathrm{SFR}_{\rm ff} = f/(t/t_{\rm ff})$. Col. (5): Theoretically estimated $\mathrm{SFR}_{\rm ff}$.

[a] Run ended with $f = 0.058$ of mass collapsed.

[b] Run ended with $f = 0.084$ of mass collapsed.

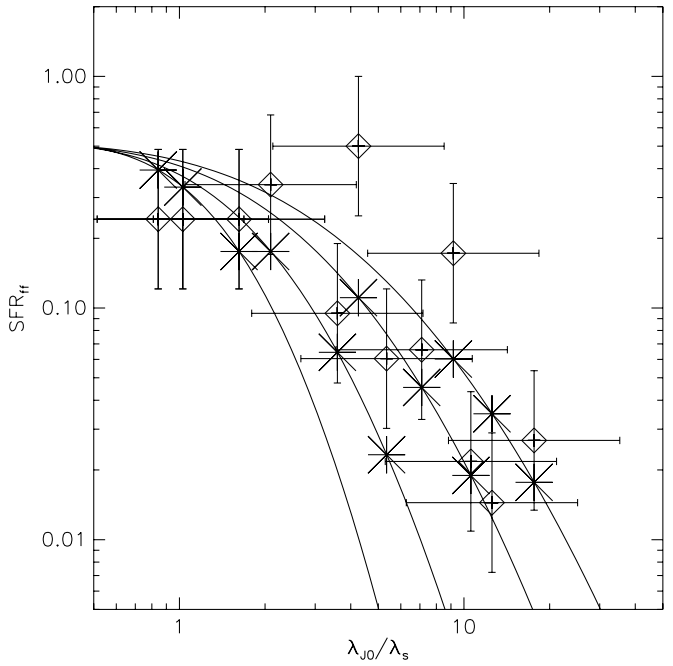

FIG. 2.—SFR per free-fall time vs. λ_{J0}/λ_s, as measured from the VBK03 runs (*error bars with diamonds*) and as predicted by our theoretical model (*asterisks*). The lines show our theoretical predictions of $\mathrm{SFR_{ff}}$ vs. λ_{J0}/λ_s for Mach numbers of 2, 3.2, 6, and 10 (*bottom to top*).

with the best-fit values in Table 1 and in Figure 2. In the figure, the simulation points have error bars corresponding to a factor of 2 uncertainty, as recommended by VBK03. As the plot shows, there is a large scatter, but we are able to reproduce the overall behavior of the VBK03 simulation data quite well. Note that $\phi_t = 1.91$ implies that, for virialized objects, the characteristic timescale is roughly a single crossing time (see § 7.7).

To understand how magnetic fields might change our results, we examine the work of Li et al. (2004), who measure the amount of mass collapsed into cores as a function of time in a magnetohydrodynamic periodic box simulation similar to those of VBK03 (identical box length, Jeans length, sound speed, and free-fall time). The initial box is magnetically supercritical, with $M/M_\Phi = 8.3$. The simulation is driven with a three-dimensional Mach number of 10 (one-dimensional Mach number $\mathcal{M} = 5.8$) at a driving wavenumber of $k = 2$ and is therefore very similar to run M6K2 in VBK03. Li et al. (2004) do not measure a sonic length, so we use the measured sonic length of $\lambda_{s3} = 0.039$ from the corresponding VBK03 run. With these parameters and our best-fit values of ϕ_x and ϕ_t, we find $\mathrm{CFR_{ff}} = 0.11$. Reading off the time at which 10% of the mass had collapsed in the highest resolution run from Figure 6 of Li et al. (2004) gives a measured $\mathrm{CFR_{ff}} = 0.072$. The simulation result is slightly lower, but well within the factor of 2 error recommended by VBK03. While this is only one simulation, it provides some confidence that the inclusion of magnetic fields in the supercritical regime will not change the SFR substantially.

2.3. $\mathrm{SFR_{ff}}$ *in Virialized Objects*

Using our theory, we can compute $\mathrm{SFR_{ff}}$ in virialized molecular clouds and clumps. Bertoldi & McKee (1992) define the virial parameter for a spherical cloud as

$$\alpha_{\rm vir} = \frac{5\sigma_{\rm tot}^2 R}{GM}, \tag{22}$$

where $\sigma_{\rm tot}$ is the one-dimensional thermal plus turbulent velocity dispersion over the entire cloud, R is the radius of the cloud, and M is the mass. Since we are concerned with large star-forming clouds that have $\sigma_{\rm tot} \gg c_s$, $\sigma_{\rm tot}$ is approximately equal to the turbulent velocity on the largest scale, which we denote σ_{2R}. Clouds with $\alpha_{\rm vir} \approx 1$ are in self-gravitating virial equilibrium, meaning that internal pressure (turbulent plus thermal) approximately balances gravity. Clouds with $\alpha_{\rm vir} \gg 1$ are non–self-gravitating and are confined by external pressure, while $\alpha_{\rm vir} \ll 1$ indicates either that the cloud is supported against gravity by a magnetic pressure larger than either the turbulent or thermal pressure, or that the cloud is undergoing free-fall collapse. We refer to objects with $\alpha_{\rm vir} \approx 1$ as "virialized."

Consider now a star-forming region that follows the line width–size relation

$$\sigma_l = \sigma_{2R}\left(\frac{l}{2R}\right)^p. \tag{23}$$

The sonic scale is therefore

$$\lambda_s = 2R\left(\frac{c_s}{\sigma_{2R}}\right)^{1/p}, \tag{24}$$

and the Jeans length at the mean density ρ_0 is

$$\lambda_{J0} = \sqrt{\frac{\pi c_s^2}{G\rho_0}} = 2\pi c_s\sqrt{\frac{R^3}{3GM}}. \tag{25}$$

Thus, the critical overdensity required for collapse is

$$x_{\rm crit} = \left(\phi_x \frac{\lambda_{J0}}{\lambda_s}\right)^2 \tag{26}$$

$$= \frac{\pi^2\phi_x^2}{15}\alpha_{\rm vir}\mathcal{M}^{2/p-2} \tag{27}$$

$$\rightarrow 1.07\mathcal{M}^2, \tag{28}$$

where $\mathcal{M} = \sigma_{2R}/c_s$ is the Mach number of the region. We have used the definition of the virial parameter given by equation (22) in the second step, and for the numerical evaluation we have used our best-fit value of ϕ_x and taken $\alpha_{\rm vir} = 1.3$. This choice is based on the evaluation of Milky Way GMCs performed by McKee & Tan (2003). We discuss it in more detail in § 7.5. From this formulation, it is straightforward using equation (20) to compute $\mathrm{SFR_{ff}}$ in a cloud in terms of $\alpha_{\rm vir}$ and $\mathcal{M}$ for the cloud. We have therefore succeeded in computing the dimensionless star formation rate $\mathrm{SFR_{ff}}$ in terms of the two basic dimensionless numbers that describe a turbulent cloud: the ratio of kinetic to potential energy (roughly $\alpha_{\rm vir}$) and the ratio of kinetic to thermal energy (roughly $\mathcal{M}^2$). This relation has an intuitive physical interpretation. At an overdensity of $x_{\rm crit}$, the thermal pressure is

$$P_{\rm th} = \rho c_s^2 \approx \rho_0\sigma_{2R}^2 = P_{\rm turb}. \tag{29}$$

Thus, the gas capable of collapse is simply the gas that is dense enough so that its thermal pressure is comparable to or greater than the mean turbulent pressure in the cloud, $P_{\rm turb}$.

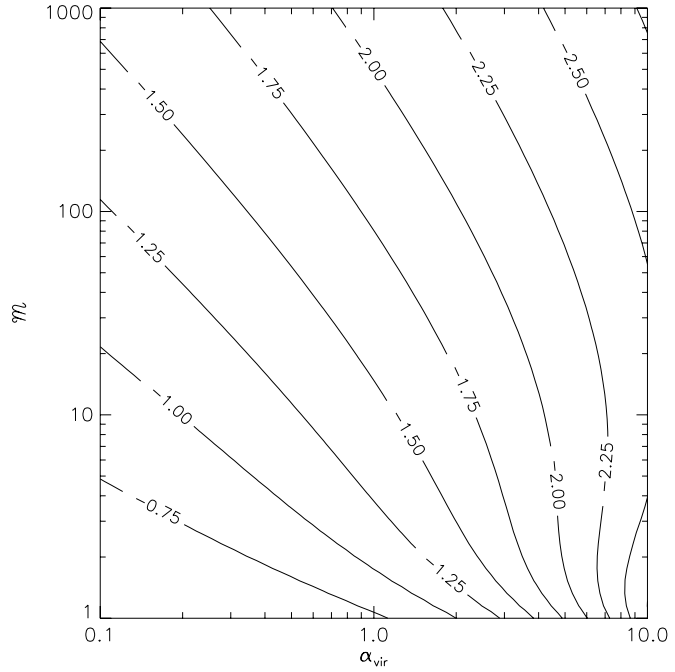

FIG. 3.—Contours of SFR per free-fall time $\mathrm{SFR_{ff}}$ vs. $\alpha_{\rm vir}$ and $\mathcal{M}$. The contours are labeled by values of $\log \mathrm{SFR_{ff}}$.

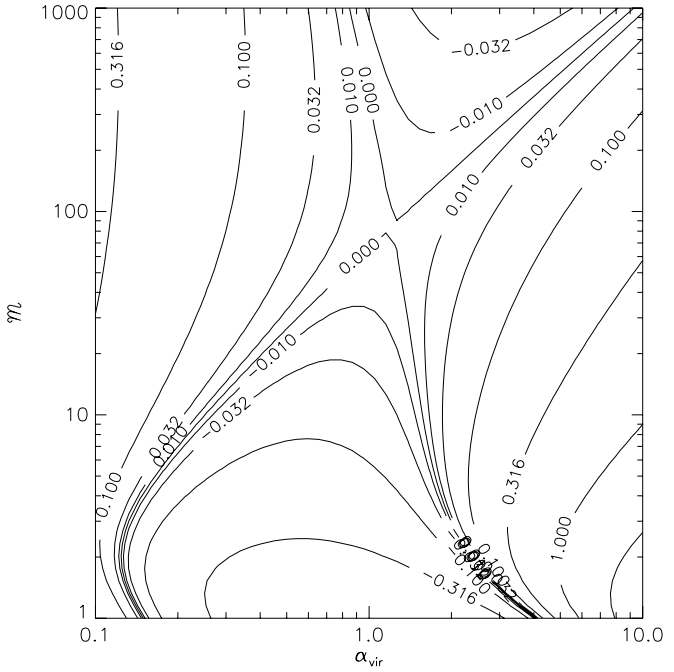

FIG. 4.—Contours of the error in our power-law fit for $\mathrm{SFR_{ff}}$, defined as error = (fit − $\mathrm{SFR_{ff}}$)/$\mathrm{SFR_{ff}}$. The labels on the contours show the value of the error.

In Figure 3 we plot the SFR per free-fall time as a function of $\alpha_{\rm vir}$ and $\mathcal{M}$ for $p = 0.5$. For convenience, we also fit $\mathrm{SFR_{ff}}$ by a power law,

$$\mathrm{SFR_{ff}} \approx 0.014 \left(\frac{\alpha_{\rm vir}}{1.3}\right)^{-0.68} \left(\frac{\mathcal{M}}{100}\right)^{-0.32}. \quad (30)$$

Figure 4 shows the error in our power-law fit as a function of $\mathcal{M}$ and $\alpha_{\rm vir}$. The error is less than 5% for values of $\alpha_{\rm vir}$ from ~0.5 to 3 and $\mathcal{M}$ from ~10 to 1000. Since real star-forming clouds generally fall within this range (see § 3), this power law is a reasonably good approximation. One important thing to note about $\mathrm{SFR_{ff}}$ is how weakly $\mathrm{SFR_{ff}}$ varies with $\mathcal{M}$. Thus, *the SFR per free-fall time in a virialized cloud depends very weakly on the Mach number of the cloud*. This is easy to understand intuitively. At fixed $\alpha_{\rm vir}$, increasing $\mathcal{M}$ increases $x_{\rm crit}$, raising the overdensity that the gas must reach to collapse. At the same time, however, increasing $\mathcal{M}$ increases the width of the PDF, putting a larger fraction of the gas at high overdensities. These two effects nearly cancel out, which is why changing $\mathcal{M}$ at fixed $\alpha_{\rm vir}$ has little effect on $\mathrm{SFR_{ff}}$.

Before proceeding, we must point out one limit of our analysis. We have assumed that the internal structure of GMCs follows the line width–size relation. However, the OB star-forming clumps observed in CS by Plume et al. (1997) do not. They have substantially higher velocity dispersions than is typical for an object of their size in their parent GMCs, and their sizes and velocity dispersions do not appear to be correlated. We interpret these clumps as regions of a GMC larger than a single core that have become gravitationally unstable and collapsed to higher surface densities and pressures than the rest of the GMC (McKee & Tan 2003), increasing their velocity dispersions. The VBK03 simulations that we have used to calibrate our model do not have enough dynamic range to include the presence of such regions, so our estimate of $\mathrm{SFR_{ff}}$ ignores their presence. Fortunately, clumps of this sort constitute only a tiny fraction of the total molecular mass of the Galaxy and are even a small fraction of the mass of their parent GMCs. Thus, the error we have made by ignoring them is negligible on the large scales with which we are concerned.

3. STAR FORMATION IN GALAXIES

In this section we usually give surface densities in units of $M_\odot\ \mathrm{pc^{-2}}$. For convenience, we note that $1\ M_\odot\ \mathrm{pc^{-2}} = 2.1\times 10^{-4}\ \mathrm{g\ cm^{-2}} = 8.9\times 10^{19}$ hydrogen nuclei $\mathrm{cm^{-2}}$, and $1\ M_\odot\ \mathrm{pc^{-2}}$ corresponds to $A_V = 0.045$ for the local dust-to-gas ratio.

3.1. *The Star Formation Law for Galactic Disks*

Our formulation applies equally well to galactic disks. The SFR per unit area of a galactic disk is simply

$$\dot{\Sigma}_* = \frac{\mathrm{SFR_{ff}} f_{\rm GMC}\Sigma_g}{t_{\rm ff}} \approx \frac{0.061}{\alpha_{\rm vir}^{0.68}} \left(\frac{f_{\rm GMC}\Sigma_g}{\mathcal{M}^{0.32} t_{\rm ff}}\right), \quad (31)$$

where Σ_g is the gas surface density of the disk, $f_{\rm GMC}$ is the fraction of it that is in molecular clouds, and $t_{\rm ff}$ and $\mathcal{M}$ are the characteristic free-fall times and Mach numbers in the star-forming regions of the disk. To estimate these quantities, we begin by considering the mean properties of galactic disks. Note that for galaxies like the Milky Way, essentially all the molecular gas is in GMCs, so $f_{\rm GMC}$ is just the molecular fraction. For starbursts, we also assume that all the molecular gas is collected into bound clouds, although this is approximate, as we discuss further in § 7.1.

Consider star formation in a galactic disk with a total surface density of $\Sigma_{\rm tot}$. The pressure at the disk midplane is then given by (cf. Elmegreen 1989; Blitz & Rosolowsky 2004)

$$P_{\rm mp} = \phi_{\rm mp}\frac{\pi}{2} G\Sigma_g\Sigma_{\rm tot} = \phi_{\rm mp} f_g^{-1}\frac{\pi}{2} G\Sigma_g^2 \equiv \phi_P \frac{\pi}{2} G\Sigma_g^2, \quad (32)$$

where $\phi_{\rm mp}$ and ϕ_P are constants of order unity and $f_g = \Sigma_g/\Sigma_{\rm tot}$ is the gas fraction in the galaxy. For an isothermal disk consisting entirely of gas, $f_g = \phi_{\rm mp} = \phi_P = 1$ exactly. For a real galactic disk containing stars, $\phi_P > 1$ because the gravity of the stars

compresses the gas. We show in Appendix A that $\phi_P \approx 3$. The scale height h_g of the gas in the disk is related to its midplane density by

$$h_g = \frac{\Sigma_g}{2\rho_g} = \frac{\sigma_g}{\sqrt{2\pi G \phi_P \rho_g}}, \tag{33}$$

where σ_g is the gas velocity dispersion. Using these two expressions to solve for the midplane density gives

$$\rho_g = \frac{\pi G \phi_P \Sigma_g^2}{2\sigma_g^2}. \tag{34}$$

To use this result, we must know σ_g, which varies from $\sim$6 km s^{-1} in normal disks (Blitz & Rosolowsky 2004) to $\sim$100 km s^{-1} in starbursts (e.g., Downes & Solomon 1998). To estimate the velocity dispersion, we assume that the star-forming part of a galaxy has a flat rotation curve with velocity $v_{\rm rot}$ and is marginally Toomre stable, so that $Q \approx 1$. Both assumptions are well satisfied in observed galaxies ranging from normal disks to starbursts and are expected on theoretical grounds (Quirk 1972; Kennicutt 1989; Navarro et al. 1997, 2004; Downes & Solomon 1998; Martin & Kennicutt 2001; Seljak 2002). The Toomre parameter Q is defined as (Toomre 1964)

$$Q \equiv \frac{\kappa \sigma_g}{\pi G \Sigma_g} = \frac{\sqrt{2}\Omega \sigma_g}{\pi G \Sigma_g}, \tag{35}$$

where $\kappa \approx \sqrt{2}\Omega$ is the epicyclic frequency, $\Omega = v_{\rm rot}/r$ is the angular velocity, and r is the galactocentric radius. We adopt $Q = 1.5$ as a typical value based on the surveys of Martin & Kennicutt (2001) and Wong & Blitz (2002). However, observed Q-values range from $\sim$0.5 up to $\sim$6, and spiral arms generally decrease Q. We discuss the resulting uncertainty in the SFR in § 7.1.

Using equation (35) to eliminate σ_g in equation (34), we obtain the mean density in a galactic disk midplane (Thompson et al. 2005),

$$\rho_g = \frac{\phi_P \Omega^2}{\pi Q^2 G} \tag{36}$$

$$\rightarrow 6.4 \times 10^{-21} Q_{1.5}^{-2} \Omega_0^2 \text{ g cm}^{-3}, \tag{37}$$

where Ω_0 is Ω in units of Myr^{-1} and $Q_{1.5} = Q/1.5$. The corresponding free-fall time in the midplane gas is

$$t_{{\rm ff},g} = \left(\frac{3\pi^2}{32}\right)^{1/2} \phi_P^{-1/2} \frac{Q}{\Omega} \tag{38}$$

$$\rightarrow 0.83 Q_{1.5} \Omega_0^{-1} \text{ Myr}. \tag{39}$$

Since the filling factor of molecular clouds is less than unity even in galaxies where the ISM is wholly molecular (Rosolowsky & Blitz 2005), the mean gas density in the star-forming clouds will be higher than this and the free-fall time lower. Let ϕ_ρ be the ratio of the mean molecular cloud density to the mean midplane density,

$$\phi_\rho \equiv \frac{\rho_{\rm cl}}{\rho_g}. \tag{40}$$

With this definition, we can write the total SFR as

$$\dot{\Sigma}_* = \left(\frac{32}{3\pi^2}\right)^{1/2} \phi_P^{1/2} \phi_\rho^{1/2} {\rm SFR}_{\rm ff} Q^{-1} f_{\rm GMC} \Sigma_g \Omega \tag{41}$$

$$\approx 0.073 \mathcal{M}^{-0.32} \phi_\rho^{1/2} Q_{1.5}^{-1} f_{\rm GMC} \Sigma_g \Omega, \tag{42}$$

where the numerical evaluation uses our fiducial values of $\alpha_{\rm vir}$ and ϕ_P. Noting that $\Omega \propto \tau_{\rm dyn}^{-1}$, we see that our formulation already gives us something like the Kennicutt-Schmidt law, equation (2). The Milky Way values for the remaining parameters are $\mathcal{M} \approx 25$ (Solomon et al. 1987), $\phi_\rho \approx 20$ (McKee 1999), $Q_{1.5} \approx 1$, and $f_{\rm GMC} \approx 0.25$ (Dame et al. 1987), which gives a numerical coefficient of 0.03 in equation (41), within a factor of 2 of the coefficient of 0.017 determined by Kennicutt (1998a) based on a large sample of galaxies. (Note that for the observational value of ϕ_ρ we are comparing the density in GMCs to the density in the spiral arms, which is a factor of $\sim$4 higher than the mean ISM density; see Nakanishi & Sofue 2003.) Thus, our theory seems consistent with the observed Kennicutt-Schmidt law. However, our results depend on two quantities, ϕ_ρ and $\mathcal{M}$, that have been directly observed only in the Milky Way and a few nearby galaxies. To completely derive a star formation law in terms of observables, we must compute ϕ_ρ and $\mathcal{M}$ in terms of other quantities. Fortunately, ϕ_ρ and $\mathcal{M}$ enter our prediction to the 0.5 and 0.32 powers, so we are relatively insensitive to errors in them.

3.2. *The Properties of Molecular Clouds*

Our goal in this section is to estimate ϕ_ρ and $\mathcal{M}$ in terms of observables. Our strategy is to treat molecular clouds as gravitationally bound fragments of the ISM in approximate virial balance. The assumption of gravitational boundedness allows us to estimate the typical mass of GMCs, and this mass plus the assumption of virial balance allow us to compute the overdensity and velocity dispersion in GMCs.

In the Milky Way, most molecular gas is in clouds with masses of a few times $10^6\ M_\odot$ (Solomon et al. 1987; Heyer et al. 2001), and the LMC shows a similar characteristic mass (Fukui et al. 2001). The typical mass is somewhat lower in M33 (Engargiola et al. 2003) and higher in M64 (Rosolowsky & Blitz 2005), indicating a very rough trend of increasing GMC mass with increasing galaxy surface density. However, all of these are ordinary disk galaxies, with surface densities $\lesssim$100 $M_\odot$ pc^{-2}. There are no observations that resolve individual molecular clouds in starbursts or ULIRGs, so we must estimate. Since GMCs appear to be gravitationally bound, they must have formed via a gravitational collapse. For this reason, their typical mass should be roughly the Jeans mass in a galactic disk (Kim & Ostriker 2001; Kim et al. 2002, 2003), giving

$$M_{\rm cl} \approx \frac{\sigma_g^4}{G^2 \Sigma_g} \tag{43}$$

$$= \frac{\pi^4 G^2 \Sigma_g^3 Q^4}{4\Omega^4} \tag{44}$$

$$\rightarrow 2.5 \times 10^3 Q_{1.5}^4 \Sigma_{g,2}^3 \Omega_0^{-4}\ M_\odot, \tag{45}$$

where in the second step we have used the definition of Q (eq. [35]) to eliminate σ_g and $\Sigma_{g,2}$ is Σ_g in units of $10^2\ M_\odot$ pc^{-2}. In the Milky Way near the solar circle, where $\sigma_g \approx 6$ km s^{-1} (consistent with the sound speed in the warm ISM; see Heiles & Troland 2003) and $\Sigma_g \approx 12\ M_\odot$ pc^{-2} (Boulares & Cox 1990), equation (43) gives $M_{\rm J} \approx 6 \times 10^6\ M_\odot$. This agrees well with

observed masses of giant atomic-molecular complexes, of which GMCs are the inner parts (Elmegreen 1989, 1994). Note that the Toomre mass and the Jeans mass are roughly equal for a disk with $Q \approx 1$. The Toomre mass is $M_{\rm T} \sim \lambda_{\rm T}^2 \Sigma_g$, where $\lambda_{\rm T} \approx Q h_g$ is the most unstable wavelength and h_g is the gas scale height. The Jeans mass is $M_{\rm J} \sim h_g^2 \Sigma_g$, so $M_{\rm T} \sim Q^2 M_{\rm J}$.

Now that we have estimated the typical masses of star-forming clouds, we can compute their typical densities from knowledge of the pressures that confine them. The pressure at the surface of a GMC is roughly the ambient pressure in the midplane of a galaxy, $P_{\rm mp}$. We define $\phi_{\overline{P}}$ as the ratio of the mean pressure in a cloud $P_{\rm cl}$ to the surface pressure, so

$$P_{\rm cl} \equiv \phi_{\overline{P}} P_{\rm mp}. \tag{46}$$

In an environment with a purely molecular ISM, this is just the ratio of the mean pressure in a gravitationally bound object to its edge pressure, and it is $\sim$2. In a predominantly atomic ISM, $\phi_{\overline{P}}$ is larger because molecular gas exists only when it is shielded by an atomic layer and the weight of the bound atomic gas increases its pressure. We estimate $\phi_{\overline{P}} \approx 10 - 8 f_{\rm GMC}$, where $f_{\rm GMC}$ is the molecular gas fraction of the galaxy, in Appendix B.

We now write down the virial theorem for a GMC, using a form of the theorem obtained by combining equation (24) of McKee (1999) with equation (A7) of McKee & Tan (2003):

$$P_{\rm cl} = \frac{3\pi}{20} \alpha_{\rm vir} G \Sigma_{\rm cl}^2, \tag{47}$$

where $\Sigma_{\rm cl}$ is the surface density of the GMC and $\alpha_{\rm vir}$ is the standard virial parameter,

$$\alpha_{\rm vir} = \frac{5\sigma_{\rm cl}^2 R_{\rm cl}}{G M_{\rm cl}} = \frac{5\sigma_{\rm cl}^2}{G\sqrt{\pi M_{\rm cl} \Sigma_{\rm cl}}}. \tag{48}$$

Equation (47) is quite intuitive, as it simply equates the GMC's internal pressure with its weight, scaled by the virial parameter as an indicator of how self-gravitating the cloud is. Together with the definition of the turbulent pressure $P_{\rm cl} = \rho_{\rm cl} \sigma_{\rm cl}^2$, equations (47) and (48) constitute three equations in the unknowns $\rho_{\rm cl}$, $\sigma_{\rm cl}$, and $\Sigma_{\rm cl}$. Solving for the molecular cloud density gives

$$\rho_{\rm cl} = \left(\frac{375}{4\pi}\right)^{1/4} \left(\frac{P_{\rm cl}^3}{\alpha_{\rm vir}^3 G^3 M_{\rm cl}^2}\right)^{1/4}, \tag{49}$$

and plugging in for $P_{\rm cl}$ and $M_{\rm cl}$ gives

$$\phi_\rho = \frac{\rho_{\rm cl}}{\rho_g} = \left(\frac{375}{2\pi^2}\right)^{1/4} \left(\frac{\phi_{\overline{P}}^3}{\phi_P \alpha_{\rm vir}^3}\right)^{1/4} \tag{50}$$

$$\rightarrow 5.0 \phi_{\overline{P},6}^{3/4}, \tag{51}$$

where $\phi_{\overline{P},6} \equiv \phi_{\overline{P}}/6$. The GMC velocity dispersion is

$$\sigma_{\rm cl} = \frac{\pi}{\sqrt{2}} \sqrt{\frac{\phi_{\overline{P}} Q^2}{\phi_\rho}} \frac{G\Sigma_g}{\Omega} \tag{52}$$

$$\rightarrow 1.6 \phi_{\overline{P},6}^{1/8} Q_{1.5} \Omega_0^{-1} \Sigma_{\rm g,2} \ {\rm km\ s^{-1}}. \tag{53}$$

The numerical evaluations are for $\phi_P = 3$ and $\alpha_{\rm vir} = 1.3$. The range of variation of ϕ_ρ with $f_{\rm GMC}$ is from $\phi_\rho = 7.3$ for $f_{\rm GMC} = 0$ to $\phi_\rho = 2.2$ for $f_{\rm GMC} = 1$. Thus, ϕ_ρ is 3–4 times larger in normal galaxies than in starbursts.

TABLE 2
FIDUCIAL PARAMETERS

Parameter	Value
$\alpha_{\rm vir}$	1.3
c_s (km s^{-1})	0.3
$\epsilon_{\rm core}$	0.5
p	0.5
ϕ_P	3.0
$\phi_{\overline{P}}$	$10 - 8 f_{\rm GMC}$
ϕ_t	1.91
ϕ_x	1.12
Q	1.5

To convert the velocity dispersion given by equation (52) to a Mach number, we must know the sound speed in the star-forming clouds. Observations of a galaxy can generally determine the temperature T in the star-forming gas, from which one can easily compute the sound speed $c_s = (k_{\rm B} T/m)^{1/2}$, where $m = 3.9 \times 10^{-24}$ g is the mean particle mass, corresponding to a fully molecular gas with a ratio of 10 H nuclei per He nucleus. However, for the purposes of numerical evaluation we can use an average sound speed. In the Milky Way, the typical temperature in star-forming clouds is $\sim$10 K (Solomon et al. 1987), giving a sound speed of 0.19 km s^{-1}. Observed starbursts have temperatures in the range 29–46 K (Gao & Solomon 2004), giving sound speeds up to 0.4 km s^{-1}. For the numerical evaluations in this paper we adopt an intermediate value of 0.3 km s^{-1}, although c_s is generally directly observable. Since the Mach number affects the SFR only through SFR$_{\rm ff}$, and SFR$_{\rm ff}$ is very insensitive to Mach number, this produces relatively little error. We therefore estimate the typical Mach numbers in star-forming regions to be

$$\mathcal{M} = \frac{\pi}{\sqrt{2}} \sqrt{\frac{\phi_{\overline{P}} Q^2}{\phi_\rho}} \frac{G\Sigma_g}{c_s \Omega} \tag{54}$$

$$\rightarrow 5.3 \phi_{\overline{P},6}^{1/8} Q_{1.5} \Omega_0^{-1} \Sigma_{g,2}. \tag{55}$$

Note that while $\sigma_{\rm cl}$ is actually the total thermal plus nonthermal velocity dispersion, star-forming regions are highly supersonic, so $\sigma_{\rm cl} \approx \sigma_{\rm nonthermal}$.

3.3. *The Full Star Formation Rate*

Using our calculated values for ϕ_ρ and $\mathcal{M}$, the SFR per unit area of a galactic disk is

$$\dot{\Sigma}_* = \frac{2^{19/8} 5^{3/8}}{3^{3/8} \pi^{5/4}} \left(\frac{\phi_P \phi_{\overline{P}}}{\alpha_{\rm vir}}\right)^{3/8} Q^{-1} {\rm SFR_{ff}} f_{\rm GMC} \Omega \Sigma_g \tag{56}$$

$$\rightarrow 9.5 f_{\rm GMC} \phi_{\overline{P},6}^{0.34} Q_{1.5}^{-1.32} \Omega_0^{1.32} \Sigma_{g,2}^{0.68} \ M_\odot \ {\rm yr^{-1}\ kpc^{-2}}, \tag{57}$$

where the numerical evaluation uses our power-law fit for SFR$_{\rm ff}$ (eq. [30]) and the fiducial values of all our other parameters, as summarized in Table 2. If one uses our approximation for $\phi_{\overline{P}}$ in terms of $f_{\rm GMC}$, this formulation of the SFR now depends solely on observables. Note that our result is different than the standard scalings with Σ_g and Ω found by Kennicutt (1998a), and it is therefore a new prediction that can be tested against future observations. Also note that this relation should apply not just on a galaxy-by-galaxy basis, but within an individual galaxy as well. This too is a new observational prediction. We discuss ways of testing these predictions in § 6.

4. COMPARISON TO THE MILKY WAY

We first test our theoretical prediction against the Milky Way. We do so in two ways to show that our results are consistent. First we use the observed properties of the molecular gas in the Milky Way plus our estimate of $\mathrm{SFR_{ff}}$, and then we use the estimated surface densities of various Milky Way components.

4.1. *Estimate from Observed GMC Properties*

Bronfman et al. (2000) estimate that the total mass of GMCs inside the solar circle is $M_{\rm mol} \approx 10^9\ M_\odot$. The mass distribution of the clouds is (Williams & McKee 1997)

$$\frac{d\mathcal{N}}{d\ln M_{\rm cl}} \approx \begin{cases} 0, & M_{\rm cl} > 6\times10^6\ M_\odot, \\ 10\left(\dfrac{M_{\rm cl}}{10^6\ M_\odot}\right)^{-0.6}, & M_{\rm cl} < 6\times10^6\ M_\odot, \end{cases} \tag{58}$$

where $M_{\rm cl}$ is the cloud mass. Solomon et al. (1987) catalog 273 Galactic GMCs observed in CO. They find that the average column density of GMCs is $N_{\rm H} \approx 1.5\times10^{22}\ \mathrm{cm^{-2}}$ independent of mass, where the subscript H indicates that we are referring to the number of hydrogen nuclei. McKee (1999) uses this result to estimate that the free-fall time in a GMC is

$$t_{\rm ff} = 4.7\left(\frac{M_{\rm cl}}{10^6\ M_\odot}\right)^{1/4}\ \mathrm{Myr}. \tag{59}$$

Combining the line width–size and mass-radius relations inferred by Solomon et al. (1987) and McKee (1999) gives a Mach number–radius relation

$$\mathcal{M}_{\rm cl} = 25\left(\frac{M_{\rm cl}}{10^6\ M_\odot}\right)^{0.25} \tag{60}$$

for a GMC temperature of 10 K. From these relations, it is straightforward to estimate the total SFR by integrating the SFR over the GMC mass distribution,

$$\dot{M}_{*,\rm pred} = \int_{10^4\ M_\odot}^{6\times10^6\ M_\odot} \mathrm{SFR_{ff}}(M_{\rm cl})\,\frac{1}{t_{\rm ff}(M_{\rm cl})}\,\frac{d\mathcal{N}}{d\ln M_{\rm cl}}\,dM_{\rm cl} \tag{61}$$

$$\approx 5.3\ M_\odot\ \mathrm{yr^{-1}}. \tag{62}$$

We have imposed a lower cutoff of $10^4\ M_\odot$ because $\alpha_{\rm vir} \gg 1$ for GMCs with smaller masses (Heyer et al. 2001), which greatly reduces their SFR. The observed SFR in the Milky Way is $\dot{M}_* \approx 3\ M_\odot\ \mathrm{yr^{-1}}$ (McKee & Williams 1997), so our estimate agrees with observations to a factor of 1.8, a reasonable fit.

An important subtlety of this analysis is that we must impose a lower cutoff when integrating the SFR over the GMC mass distribution because small clouds, if they are virialized, contribute significantly to the SFR. The integrand in equation (61) scales as roughly $M_{\rm cl}^{-0.93}$: one gets an exponent of -0.6 from the logarithmic mass spectrum $d\mathcal{N}/d\ln M_{\rm cl}$, -0.25 from the free-fall time, and approximately -0.08 from the dependence of $\mathrm{SFR_{ff}}$ on the Mach number and hence on $M_{\rm cl}$. Thus, each decade range in the mass of virialized clouds contributes almost equally to the SFR. The contribution to the total SFR from small clouds is small not because the clouds contain a small amount of mass, but because small clouds are not virialized.

4.2. *Estimate from Surface Densities*

We can also compute the Milky Way SFR using surface densities, the rotation curve, and the velocity dispersion. The vast majority of star formation in the Milky Way occurs in a ring from 3 to 11 kpc in Galactocentric radius (McKee & Williams 1997) within which the molecular and atomic gas surface densities are roughly (Wolfire et al. 2003)

$$\Sigma_{\rm mol} \approx \begin{cases} 6.3\exp\left[\dfrac{-(r_k-4.85)^2}{(2)2.25^2}\right]\ M_\odot\ \mathrm{pc^{-2}}, & 3 \le r_k < 6.97, \\ 4.1\exp\left[\dfrac{-(r_k-6.97)}{2.89}\right]\ M_\odot\ \mathrm{pc^{-2}}, & r_k \ge 6.97, \end{cases} \tag{63}$$

and

$$\Sigma_{\rm H\,I} \approx \begin{cases} (2.0r_k - 0.8)\ M_\odot\ \mathrm{pc^{-2}}, & r_k < 4, \\ 7\ M_\odot\ \mathrm{pc^{-2}}, & 4 \le r_k < 8.5, \\ \left[-1.57 + 8.57\left(\dfrac{r_k}{8.5}\right)\right]\ M_\odot\ \mathrm{pc^{-2}}, & r_k > 8.5, \end{cases} \tag{64}$$

where r_k is the galactocentric radius in kpc and we have multiplied the Wolfire et al. (2003) values for the surface density of hydrogen by 1.4 to get the total surface density including both H and He. From these surface densities we can directly compute Σ_g, $f_{\rm GMC}$, and ϕ_ρ. The Galactic rotation speed is $v_{\rm rot} \approx 220\ \mathrm{km\ s^{-1}}$ and is flat over the ring (Binney & Merrifield 1998), so

$$\Omega = \frac{0.22}{r_k}\ \mathrm{Myr^{-1}}. \tag{65}$$

The temperature in the molecular gas is $\sim$10 K (Solomon et al. 1987), giving a sound speed $c_s \approx 0.2\ \mathrm{km\ s^{-1}}$. We estimate $\mathcal{M}$ as a function of radius from Σ_g and Ω using equation (54).

The final step is to estimate Q, which we do in two different ways. First, we compute Q from Σ_g assuming that the gas velocity dispersion is $\sigma_g = 6\ \mathrm{km\ s^{-1}}$ independent of radius. This is consistent with observations (Kennicutt 1989; Heiles & Troland 2003), although the observations are quite uncertain because it is difficult to determine the velocity dispersion as a function of radius within the Galaxy. Second, we compute Q from the gas scale height, which can be directly measured in the Milky Way. Equation (33) allows us to compute ρ_g from Σ_g and h_g, and equation (36) gives Q in terms of ρ_g and Ω. The scale heights of the atomic and molecular gas within the star-forming ring are (Wolfire et al. 2003)

$$h_{\rm H\,I} \approx \begin{cases} 65\ \mathrm{pc}, & r_k < 8.5, \\ 65\exp\left(\dfrac{r_k-8.5}{6.7}\right)\ \mathrm{pc}, & r_k \ge 8.5, \end{cases} \tag{66}$$

and

$$h_{\rm mol} \approx \begin{cases} 33\ \mathrm{pc}, & r_k < 8.5, \\ 33\exp\left(\dfrac{r_k-8.5}{6.7}\right)\ \mathrm{pc}, & r_k \ge 8.5. \end{cases} \tag{67}$$

Note that we have converted the half-density heights given by Wolfire et al. (2003) to scale heights by assuming an isothermal density profile $\rho \propto \mathrm{sech}^2\,[z/(2h_g)]$. We determine a Q by computing the midplane density of atomic and molecular gas and then solving equation (36) for Q using the surface density–weighted average of the two midplane densities. The result agrees to

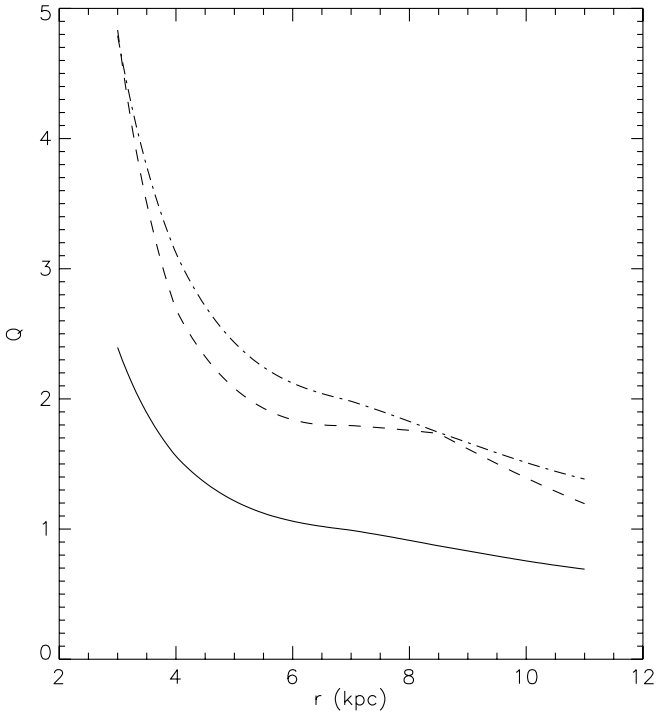

FIG. 5.—Predicted value of Q vs. radius, estimated using azimuthal averages and scale heights (*dot-dashed line*), using azimuthal averages and $\sigma_g = 6$ km s^{-1} (*dashed line*), and corrected for spiral structure (*solid line*).

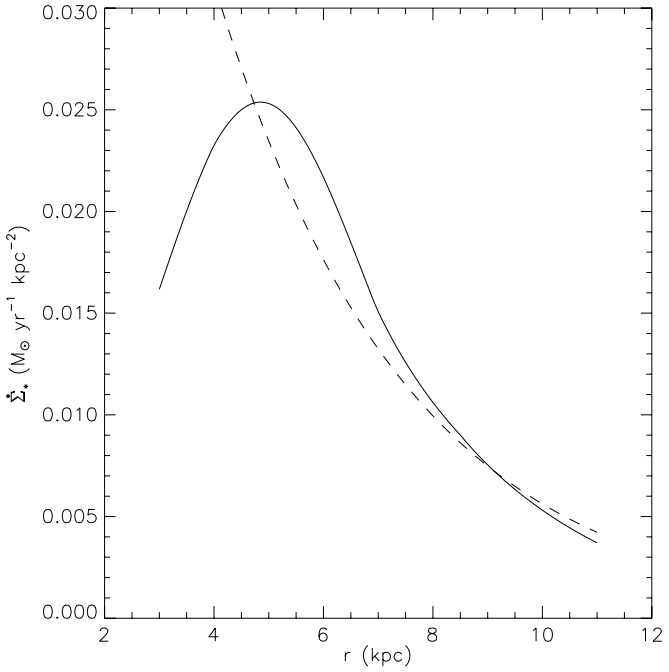

FIG. 6.—Predicted variation in the SFR per unit area, $\dot{\Sigma}_*$, with galactocentric radius r. The solid line is our model, and the dashed line is the model of McKee & Williams (1997), scaled to have the same integrated SFR that we predict.

within 20% with the value Q as a function of radius we derive using the first method. We plot the azimuthally averaged Q versus radius for the Milky Way in Figure 5. However, most Milky Way star formation occurs in the spiral arms. Balbus (1988) shows that the local Q-value in a spiral arm is related to the azimuthally averaged Q by

$$Q_{\rm arm} \approx Q_{\rm avg}\left(\frac{\Sigma_{\rm arm}}{\Sigma_{\rm avg}}\right)^{-1/2}. \tag{68}$$

The Milky Way's spiral arms are overdense by factors of $\sim$4 (Nakanishi & Sofue 2003), so we reduce our estimated value of Q by a factor of 2 to account for this effect. We also show the corrected Q in Figure 5.

Integrating over the star-forming ring, we find a predicted SFR

$$\dot{M}_{*,\,\rm pred} \approx \int_{3\ \rm kpc}^{11\ \rm kpc} 9.5 f_{\rm GMC}\phi_{\bar{P},6}^{0.34} Q_{1.5}^{-1.32}\Omega_0^{1.32} \times \Sigma_{g,2}^{0.68} 2\pi R\, dR\ M_\odot\ {\rm yr}^{-1}\ {\rm kpc}^{-2} \tag{69}$$

$$\approx 4.5\ M_\odot\ {\rm yr}^{-1}. \tag{70}$$

This agrees with the observed SFR of 3 $M_\odot$ yr^{-1} in the Milky Way (McKee & Williams 1997) and with our estimate based on observed GMC properties to better than a factor of 2. If we omit the correction for spiral arms, we get an SFR of 2.1 $M_\odot$ yr^{-1}, still in good agreement, so the spiral arm correction is not critical.

Note that equation (69) gives a prediction not just for the total SFR in the Galaxy but also for the radial distribution of star formation. We show this in Figure 6. For comparison, we also show the model of McKee & Williams (1997) (scaled to have the same integrated SFR as ours), which is generally consistent with observational data on the radial distribution of star formation outside 4 kpc. Our model is similar to the McKee & Williams (1997) model in this range but differs substantially inside 4 kpc because McKee & Williams (1997) use a simple exponential distribution with a cutoff for the radial variation of the molecular gas surface density, while we use a more accurate distribution that better reflects the decline in the molecular gas surface density in the inner Galaxy. We find that the characteristic radius of star formation in the Milky Way, defined as the radius within which half the star formation occurs, is $R_{\rm char} \approx 7.1$ kpc. Taking the outer radius of the star-forming disk to be 11 kpc, this gives $R_{\rm char} = 1.3R_{1/2}$. This suggests that the common observational practice of measuring quantities such as angular velocities at half the outer radius of star formation (Kennicutt 1998b) should be reasonably accurate.

5. COMPARISON TO GALACTIC-AVERAGE STAR FORMATION RATES

5.1. *Statistical Comparison*

For a second test we compare our prediction against a sample of 95 galaxies, taken from the normal galaxies and starbursts compiled by Kennicutt (1998a) plus starbursts from Downes & Solomon (1998). For the Kennicutt galaxies, we use the measured values of $\Sigma_{\rm mol}$, Σ_g, and $\tau_{\rm dyn}$ as reported in Tables 1 and 2 of Kennicutt (1998a) to compute a theoretical SFR from equation (56). We follow Kennicutt in taking $\Omega = 4\pi/\tau_{\rm dyn}$ to be the typical value of Ω in the star-forming region, and we exclude galaxies for which there is no measured value of $\tau_{\rm dyn}$. For starbursts where there is no measured value of Σ_g (only $\Sigma_{\rm mol}$) we assume $f_{\rm GMC} = 1$.

For the Downes & Solomon (1998) sources, we use a compilation of supporting information from T. Thompson (2005, private communication). As with the Kennicutt starbursts, we take $f_{\rm GMC} = 1$ for all these points. We derive Σ_g and $\tau_{\rm dyn}$ from the gas mass, half-power radii, and rotation curves from Tables 4, 5, and 9 of Downes & Solomon (1998), and we derive SFRs from the far-infrared (FIR) luminosities taken from the texts of Downes & Solomon (1998; IRAS 00057+4021, IRAS 02483+4302, VII Zw 31), Genzel et al. (2001; IRAS 23365+3604, IRAS 17208−0014), Heckman et al. (2000; IRAS 10565+2448), and Soifer et al.

(2000; Mrk 231). We compute the SFRs from the FIR luminosities using the conversion factor of Kennicutt (1998b). The data set includes multiple points for Arp 193, Mrk 273, and Arp 220 because Downes & Solomon (1998) break the sources up into a more diffuse component and one or two "extreme" starburst nuclei. For these objects we include both the diffuse component and the nucleus or nuclei. Data for the surface densities, dynamical times, and luminosities for the diffuse components come from Tables 4, 5, and 9 and the text of Downes & Solomon (1998), while data for the nuclei come from Table 12.

To compare to this sample, we compute

$$\chi^2 \equiv \frac{1}{N_{\rm data} - N_{\rm fit}} \sum \left[\log\left(\dot{\Sigma}_{*,\rm data}\right) - \log\left(\dot{\Sigma}_{*,\rm theory}\right)\right]^2 \quad (71)$$

for our model and, as a normalization, for the Kennicutt (1998a) empirically determined best fit. The number of fit parameters $N_{\rm fit}$ is unity for the Kennicutt best fit and zero for our model. We find $\chi^2 = 0.40$ for the best fit of Kennicutt (1998a), while our theoretical model gives $\chi^2 = 0.55$. Note that these are not traditional χ^2 goodness-of-fit statistics, since we are using the logarithm of the data, we have no error bars for the measurements, and the dominant errors (arising from extinction, an imperfectly known IMF, and similar astrophysical uncertainties; see Kennicutt 1998b) are systematic and therefore highly non-Gaussian. Instead, the meaning of this statistic is that 10^{χ} is the rms factor by which the model errs in estimating the SFR. Thus, our results correspond to rms errors of a factor of 5.6 for our model and a factor of 4.3 for the Kennicutt fit. Given the factor of several systematic uncertainties in the measured SFRs, these values are essentially identical.

5.2. *The Kennicutt-Schmidt Law*

The Kennicutt-Schmidt law correlates the SFR with either $\Sigma_g\Omega$ or Σ_g, while our theory makes a prediction based on Σ_g, Ω, and $f_{\rm GMC}$. From an intuitive physical standpoint, one would be surprised if the SFR did not depend on all three of our parameters to at least some degree. Thus, the two forms of the Kennicutt-Schmidt law represent two ways of projecting a four-dimensional space (consisting of Σ_g, Ω, $f_{\rm GMC}$, and $\dot{\Sigma}_*$) onto two dimensions. To compare our theory directly to these laws, as opposed to the underlying data as we did in § 5.1, we must make some additional approximations. We stress that we make these approximations only for the purposes of the projection and that the right way to test our theory is to use the measured values of Σ_g, Ω, and $f_{\rm GMC}$, as we did in § 5.1. We make them because they allow us to show, in a relatively intuitive manner, why projecting the four-dimensional data down to two dimensions still allows such a good fit to the observations.

Since neither version of the Kennicutt-Schmidt law involves $f_{\rm GMC}$, we must estimate it in terms of Σ_g or Ω. Wong & Blitz (2002) and E. Rosolowsky & L. Blitz (2005, in preparation) find that the ratio of molecular to atomic gas follows the approximate relation

$$\frac{\Sigma_{\rm mol}}{\Sigma_{\rm H\,I}} \approx \left(\frac{P_{\rm mp}/k_{\rm B}}{2.5\times10^4\ {\rm cm^{-3}\ K}}\right)^{1.0}, \quad (72)$$

with about half a dex of scatter. Since $P_{\rm mp}$ is just a function of Σ_g in our model, equation (72) gives

$$f_{\rm GMC} \approx \left(1 + 0.025\Sigma_{g,2}^{-2}\right)^{-1}, \quad (73)$$

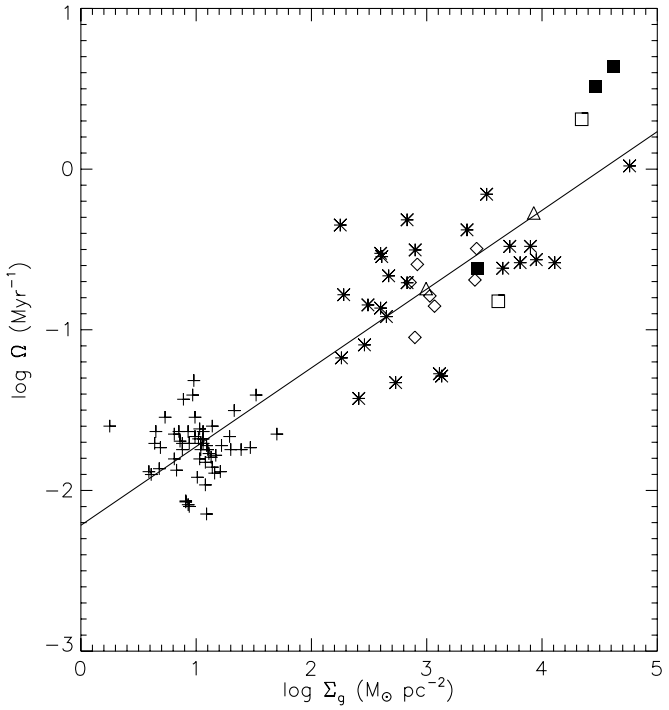

FIG. 7.—Σ_g vs. Ω for observed galaxies. The data points represent normal disks (*plus signs*), circumnuclear starbursts (*asterisks*), ULIRGs (*diamonds*), Arp 193 (*triangles*), Mrk 273 (*open squares*), and Arp 220 (*filled squares*). For a description of how we derived these data points, see § 5.1. The line shows a linear fit to the data.

for our fiducial $\phi_P = 3$. Note that most of the dynamic range of the Kennicutt-Schmidt law lies above $\Sigma_g = 100\,M_\odot\,{\rm pc}^{-2}$, for which $f_{\rm GMC} \gtrsim 0.98$, where we have made the approximation that most molecular gas is in GMCs. Thus, $f_{\rm GMC}$ is almost constant over most of the range of the Kennicutt-Schmidt law, which is part of the reason that a projection of the data that neglects $f_{\rm GMC}$ makes little difference.

With $f_{\rm GMC}$ approximated in terms of Σ_g, the remaining step is to project from the three-dimensional space of $\dot{\Sigma}_*$, Σ_g, and Ω onto a two-dimensional space of $\dot{\Sigma}_*$ and just Σ_g or $\Sigma_g\Omega$. To do this, we make use of the fact that Σ_g and Ω for galaxies appear to be correlated, as shown in Figure 7. The correlation is fitted reasonably well by the rule

$$\Omega_0 = 0.058\Sigma_{g,2}^{0.49}, \quad (74)$$

as the figure shows. We can use this rule to estimate Σ_g and Ω independently from any combination of Σ_g and Ω, allowing us to project our theory into the same lower dimensional space as the Kennicutt-Schmidt law. This correlation is the other half of the reason that projecting the data into two dimensions works well: Σ_g and Ω are not really independent, at least in the available data set. Because they are correlated, projecting the data onto any appropriately chosen combination of them will work, which is why the $\Sigma_g^{1.4}$ and $\Sigma_g\Omega$ forms of the Kennicutt-Schmidt law work equally well, as does our prediction, which is approximately $\dot{\Sigma}_* \propto \Sigma_g^{0.68}\Omega^{1.32}$. Even though the parameter space is four-dimensional, most of the data points lie near a line within it, which makes distinguishing different models quite difficult. We discuss how to break this degeneracy in § 6. Also note, however, that while equation (74) holds between galaxies, it is unknown if it holds within galaxies. For this reason, the projection we derive to compare to the Kennicutt-Schmidt law may apply only to averages over many galaxies, not within individual galaxies.

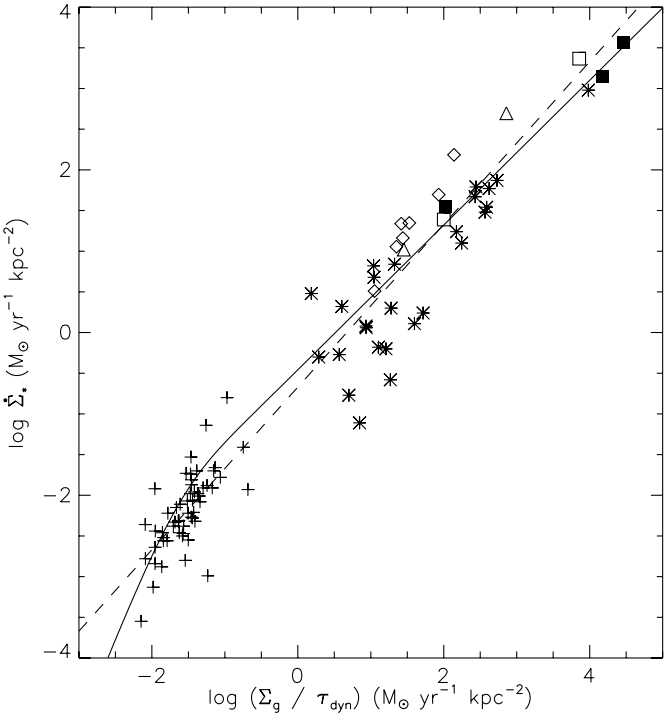

FIG. 8.—Predicted SFR vs. $\Sigma_g/\tau_{\rm dyn}$ (*solid line*). We also plot the Kennicutt (1998b) best fit (*dashed line*) and observed points for normal galaxies from Kennicutt (1998a; *plus signs*), circumnuclear starbursts from Kennicutt (1998a; *asterisks*), ULIRGs (*diamonds*), Arp 193 (*triangles*), Mrk 273 (*open squares*), and Arp 220 (*filled squares*). For a description of how we derived these data points, see § 5.1.

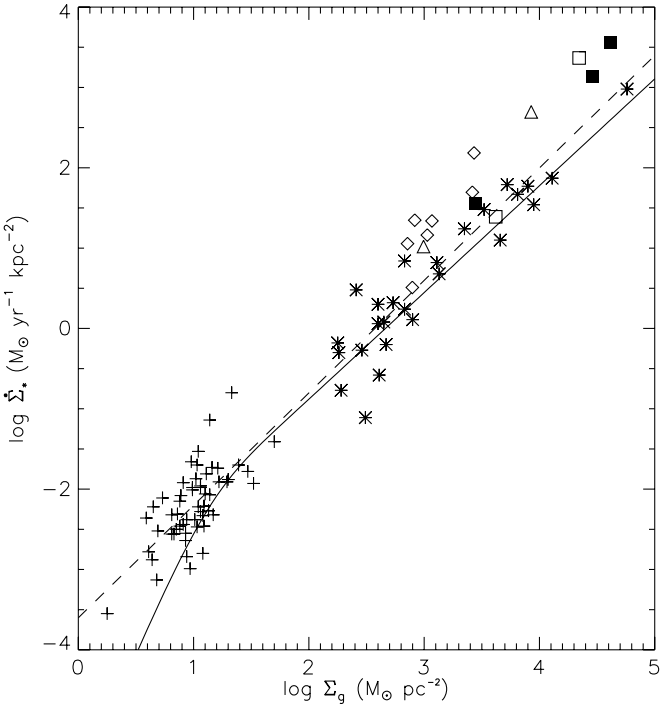

FIG. 9.—Predicted SFR vs. Σ_g (*solid line*). We also plot the Kennicutt (1998b) best fit (*dashed line*). The data points are observed galaxies: normal disks (*plus signs*), circumnuclear starbursts (*asterisks*), ULIRGs (*diamonds*), Arp 193 (*triangles*), Mrk 273 (*open squares*), and Arp 220 (*filled squares*). For a description of how we derived these data points, see § 5.1.

Using equations (73) and (74) in equation (56), our theoretical prediction for the SFR in terms of $\Omega\Sigma_g$ is

$$\dot{\Sigma}_* \approx 3.2\phi_{\overline{P},6}^{0.34} Q_{1.5}^{-1.32} f_{\rm GMC} \left(\Omega_0 \Sigma_{g,2}\right)^{0.89} M_\odot \ {\rm yr}^{-1} \ {\rm kpc}^{-2}, \quad (75)$$

where

$$f_{\rm GMC} \approx \left[1 + 5.5\times10^{-3}\left(\Omega_0\Sigma_{g,2}\right)^{-1.34}\right]^{-1} \quad (76)$$

and $\phi_{\overline{P}} \approx 10-8 f_{\rm GMC}$. The observed Kennicutt-Schmidt law with this choice of dependent variable is (Kennicutt 1998a)

$$\dot{\Sigma}_* = 0.017\Omega\Sigma_g. \quad (77)$$

We plot this and our theoretical prediction in Figure 8. As the plot shows, our theoretical prediction, when we take into account the way that $f_{\rm GMC}$, Σ_g, and Ω are related, essentially reproduces the first form of the Kennicutt-Schmidt law. If we instead choose Σ_g to be our independent variable, following the second form of the Kennicutt-Schmidt law, our theoretical prediction is

$$\dot{\Sigma}_* = 0.19\phi_{\overline{P},6}^{0.34} Q_{1.5}^{-1.32} f_{\rm GMC} \Sigma_{g,2}^{1.33}, \quad (78)$$

where $f_{\rm GMC}$ is given by equation (73) and $\phi_{\overline{P}}$ is approximated in terms of $f_{\rm GMC}$ as for the previous case. The observed law is (Kennicutt 1998a)

$$\dot{\Sigma}_* = (2.5 \pm 0.7)\times10^{-4}\left(\frac{\Sigma_g}{1\ M_\odot\ {\rm pc}^{-2}}\right)^{1.4\pm0.15} M_\odot \ {\rm yr}^{-1} \ {\rm kpc}^{-2} \quad (79)$$

$$\approx 0.16\Sigma_{g,2}^{1.4} \ M_\odot \ {\rm yr}^{-1} \ {\rm kpc}^{-2}. \quad (80)$$

We plot this and our theoretical prediction in Figure 9 and find that, again, our fit is reasonably good. The only exception is at values of $\Sigma_g \lesssim 1\ M_\odot\ {\rm pc}^{-2}$. The error there arises from the fact that almost all the galaxies with Σ_g so small lie well above the Ω versus Σ_g correlation we have used to project our theory (as shown in Fig. 7), so the values of Ω we are using are systematically smaller than those of the real galaxies in that region of parameter space. Since our SFR depends on $\Omega^{1.32}$, this underestimation of Ω causes the theory to underpredict the SFR. If one uses the measured values of Ω rather than the linear fit, the error at small Σ_g is no larger than it is elsewhere.

6. FUTURE OBSERVATIONAL TESTS

Our theory makes three observational predictions that should be directly testable in the next few years. First, we can test our theory on nearby galaxies where molecular clouds are directly observable. In § 4.1 we compute the SFR in the Milky Way by integrating over the observed distribution of Milky Way GMCs. While we have some information about larger GMCs in nearby galaxies, small GMCs make a nonnegligible contribution to the SFR there just as they do in the Milky Way. To reliably compute the SFR in another galaxy, we must therefore identify the lower mass cutoff below which molecular clouds become nonvirialized. This cutoff has not yet been observed in any galaxy but the Milky Way, but such an observation is a straightforward extension of existing data sets to higher sensitivities and angular resolutions. It should be within the capabilities of the SMA, CARMA, or ALMA. Once one has determined the full cloud mass distribution for another galaxy down to the nonvirial cutoff, one can compute the SFR in another galaxy by using equation (21) to compute the SFR in each cloud, just as we have done for the Milky Way. Since this type of test depends only on our calculation of $\rm SFR_{ff}$ and not on any of our calculations of GMC properties in external

galaxies, this method allows our theory of $\mathrm{SFR_{ff}}$ to be tested independently of the rest of our model.

Observations that resolve the SFR in a galaxy in annular rings but cannot resolve individual GMCs provide a second possible test of our theory. With sufficiently good data, one could use equation (57) to predict the SFR versus radius within a galaxy, just as we have done for the Milky Way in § 4.2. This could then be compared to resolved observations of star formation versus radius, similar to those of Wong & Blitz (2002). The primary observational challenge in this comparison is that, to compare to a single galaxy where one cannot assume that parameters such as Q have their average values, one must measure all the information that we measured for the Milky Way. In particular, one must know Σ_g, $f_{\rm GMC}$, Ω, and Q as a function of radius. The first three are relatively straightforward, but measuring Q requires that one be able to measure either the velocity dispersion or the gas scale height. Neither quantity is easy to determine observationally, but without it the theoretical predictions will be uncertain by a factor of several. We suggest two possible ways to make this measurement. First, one could perform resolved observations of a starburst galaxy, where σ_g is large enough to be comparable to the galactic rotation velocity and is therefore easier to measure. Second, one could measure σ_g in a normal disk that is face-on and then use the Tully & Fisher (1977) relation to obtain a rotation velocity. Since there is some scatter in the Tully-Fisher relation, this procedure would likely need to be performed over several galaxies to minimize the errors arising from the uncertainty in the rotation curve.

A third possible test involves using a sample of galaxies similar to but larger than that in Kennicutt (1998a). We found in § 5.2 that, because Σ_g and Ω are themselves correlated, $\dot{\Sigma}_*$ will correlate equally well with an infinite number of combinations of Σ_g and Ω. Our theory predicts that the true scaling should be $\dot{\Sigma}_* \propto f_{\rm GMC}\Sigma_g^{0.68}\Omega^{1.32}$, but the current data cannot distinguish this combination of Σ_g and Ω from any other. However, there is no reason that a future, larger sample of galaxies could not. In order to break the degeneracy between combinations of Σ_g and Ω, a future sample must contain a large number of galaxies, or annuli within galaxies, with fixed Σ_g and varying Ω, or fixed Ω and varying Σ_g. With such a sample, one could compute predicted SFRs using equation (57) and repeat our analysis in § 5.1 and determine whether $\Sigma_g^{0.68}\Omega^{1.32}$ is a better fit. However, there is likely to be considerable scatter arising from the stochastic nature of the cloud and star formation process. This test will therefore require a considerably larger sample of galaxies than are currently available.

Finally, note that one cannot easily test our theory by looking at individual GMCs. Simulations of turbulence-regulated star formation show significant fluctuations in the SFR versus time, and we expect that real GMCs will also have large fluctuations. Thus, our theory is valid only as an average over an ensemble of GMCs. Furthermore, observations of a single GMC run into a problem with GMC ages. Tracers of star formation such as FIR and radio continuum luminosities measure the mass of stars formed over some period in the past. The amount of time depends on the tracer, but even tracers sensitive only to the very youngest stellar populations integrate the star formation over several million years. We do not know the GMC lifetime well, and even in our model of virialized GMCs we cannot rule out the possibility that it is only $\sim$10 Myr, a few GMC crossing times. Thus, one cannot be confident when observing a single GMC that it has been forming stars for long enough to have reached a steady state luminosity in the tracer that one is using. This makes observations difficult to interpret because one cannot break the degeneracy between the SFR and the age of the cloud.

7. DISCUSSION

7.1. *Estimate of Uncertainties*

We begin to estimate our uncertainties by considering how much our estimates of the SFR could be off by considering a "worst-case scenario" for our unknown parameters, $\alpha_{\rm vir}$, ϕ_P, $\phi_{\overline{P}}$, Q, and $\epsilon_{\rm core}$. Our fiducial value for $\alpha_{\rm vir}$ is 1.3, and a plausible range based on the observations is 1–2. As discussed in Appendices A and B, the plausible ranges in ϕ_P and $\phi_{\overline{P}}$ are $\phi_P = 1$–6 and $\phi_{\overline{P}} = 2$–10. We have also used a fiducial value of $Q = 1.5$. Simulations of purely gaseous magnetized disks show that collapse in a disk can set in at Q in the range 0.9–1.6 (Kim & Ostriker 2001; Kim et al. 2002, 2003). Analytic work shows that stars allow smaller values of Q to be stable (Jog & Solomon 1984; Rafikov 2001). Observationally, most galaxies fall in the range $Q = 0.75$–3 (Martin & Kennicutt 2001; Wong & Blitz 2002), with outliers going as far as $Q = 0.5$–6. We adopt $Q = 0.75$–3 as our plausible range of variation for most galaxies. Finally, we have taken $\epsilon_{\rm core} = 0.5$, but the plausible range for the mass fraction ejected by feedback is $\epsilon_{\rm core} = 0.25$–0.75 (Matzner & McKee 2000).

If we consider all of these parameters simultaneously assuming their extreme values, for a given galaxy we can reduce our predicted SFR by as much as a factor of 10 and increase it by as much as a factor of 6, relative to our fiducial case given by the parameters in Table 2. A more realistic estimate of the error is probably a factor of $\sim$3 because there is no reason our errors should add up systematically in this fashion. Indeed, the maximum errors are possible only for combinations of parameters that can be ruled out on observational grounds other than the Kennicutt-Schmidt law. For example, a reduction of the SFR by a factor of 10 is possible only if $\phi_{\overline{P}} = 2$, $\phi_P = 6$, and $\alpha_{\rm vir} = 2$, giving $\phi_\rho = 1.3$. This corresponds to a galaxy where molecular clouds are only overdense relative to the mean in the ISM by 30%. No known galaxy, including ones where the ISM is entirely molecular, has clouds with such a small overdensity compared to the rest of the ISM. Indeed, such a galaxy would effectively have no clouds at all, just a continuous intercloud medium. Similarly, an increase in the SFR by a factor of 6 occurs for $\phi_{\overline{P}} = 10$, $\phi_P = 1$, and $\alpha_{\rm vir} = 1$. Plugging in Milky Way values of Ω and Σ_g with these parameters gives $\mathcal{M} \approx 5$, much smaller than the observed velocity dispersion in GMCs in the Milky Way or in any other galaxy.

We can also identify a number of uncertainties not associated with any specific parameters, but instead with conceptual assumptions that we have made. First, observations have confirmed that, in at least some clouds, the SFR is lower in the outer than the inner parts (Li et al. 1997; Johnstone et al. 2004), perhaps due to increased ionization there (McKee 1989). The periodic box simulations we have used to calibrate $\mathrm{SFR_{ff}}$ do not include any effects arising from the finite size of real GMCs, and this may produce an error. A second effect is that we have assumed that all the gas in starbursts is in bound structures capable of forming stars. However, observed galactic nuclei and starbursts that are molecular throughout consist of a collection of clouds with a molecular intercloud medium (Solomon et al. 1997; Rosolowsky & Blitz 2005). Our assumption that all the gas is in bound structures may therefore cause us to systematically overestimate the SFR. However, Rosolowsky & Blitz (2005) find that in M64 the clouds account for $\sim$75% of the mass, and simulations such as those of VBK03 show that

$\gtrsim$50% of the mass does collapse in unstable environments, so the error is probably small. Third, we have neglected magnetic fields. We argue in § 7.3 that star-forming clouds are likely magnetically supercritical and thus cannot be held up against collapse by magnetic fields, and we present preliminary evidence in § 2.2 that a magnetic field in a fairly supercritical cloud does not substantially inhibit star formation. However, it is possible that a magnetic field stronger than the one used in Li et al. (2004), yet still not strong enough to make the cloud subcritical, could inhibit the formation of cores by preventing gas from flowing across field lines to accrete onto them. We find this unlikely, however, since in a supercritical cloud the Alfvén Mach number is likely to be unity or greater. Fourth, we have ignored the possible effects of star formation in objects like the clumps observed by Plume et al. (1997) that do not lie on the line width–size relation and that numerical simulations thus far lack the resolution to model. Since these objects are overpressured and overdense compared to typical Galactic star-forming clouds, they have shorter free-fall times and form stars faster. By neglecting them, we probably systematically underestimate the SFR. The extent of the underestimate is somewhat uncertain, since simulations to date have not modeled this effect, and we do not know exactly how much mass is in these clumps in the Galaxy.

7.2. *Application to Simulations*

Our theory of turbulence-regulated star formation is readily applicable to simulations on cosmological or galactic scales that do not have enough resolution to model molecular cloud formation or star formation directly. This is particularly true because, while we can integrate over an entire galactic disk to compute average SFRs, we also predict the SFR in terms of local properties of the gas.

In a simulation, one usually wants to implement star formation as a subgrid model. This requires a recipe for determining at what rate the mass in a given cell or particle is transformed into stars. Equation (21) gives the SFR in terms of the local free-fall time $t_{\rm ff}$, molecular mass $M_{\rm mol}$, and the SFR per free-fall time $\mathrm{SFR}_{\rm ff}$, which is a function of $\alpha_{\rm vir}$ and $\mathcal{M}$, the local virial parameter and Mach number. Since in a simulation the density of every cell is generally known, it is simple to compute $t_{\rm ff}$. Since the gas mass but not the molecular mass of every cell is known, one must determine $f_{\rm GMC}$ to find $M_{\rm mol}$. To do this, one may either assume that sufficiently dense cells are entirely molecular or more directly use the observed relation between pressure and $f_{\rm GMC}$, equation (72). (One should be wary of applying this rule to galaxies with metallicities too different from that of the Milky Way, however, since the correlation almost certainly has some metallicity dependence.)

Finally, to compute $\mathrm{SFR}_{\rm ff}$, one needs to know the virial parameter and Mach number within a cell. The easiest way to estimate $\mathcal{M}$ is to compute the velocity dispersion over a small region around the cell and extrapolate down to the size of the cell using the line width–size relation $\sigma \propto l^{0.5}$. This plus the temperature of the cell yields $\mathcal{M}$ within the cell. While this procedure is somewhat uncertain because it requires extrapolation to scales below the grid size, $\mathcal{M}$ has only a weak effect on $\mathrm{SFR}_{\rm ff}$. One can compute $\alpha_{\rm vir}$ by using $\mathcal{M}$ to estimate the kinetic energy in the cell and comparing to the estimated gravitational self-energy of the cell. This process for estimating $\alpha_{\rm vir}$ is similar to the process of estimating whether a region is bound used in the sink particle creation procedures outlined by Bate et al. (1995) for Lagrangian codes and Krumholz et al. (2004) for Eulerian codes. From $\alpha_{\rm vir}$ and $\mathcal{M}$, one can compute $\mathrm{SFR}_{\rm ff}$, and from that $\dot{M}_*$.

This procedure provides a simple estimate for the rate at which a cell turns its mass into stars that is based on a physical model rather than an arbitrary density cutoff and efficiency for star formation, which are commonly used in simulations now. One caveat on our approach, however, is that it does not apply to primordial star formation, where the primary limit on star formation is the ability of the gas to cool, rather than turbulent support.

7.3. *Magnetic Fields*

Our theory of star formation regulated by supersonic turbulence is only valid if star formation occurs primarily in regions that are magnetically supercritical. If molecular clouds are magnetically subcritical, then magnetic fields can prevent collapse, and the time required for the flow to "replace" collapsing cores is the ambipolar diffusion time rather than the free-fall time. This effect could inhibit flow in unbound regions of GMCs even if the clouds overall are supercritical. However, our comparison with the work of Li et al. (2004) gives preliminary evidence that this effect is small.

Both observations and general theoretical considerations support the idea that molecular clouds are supercritical. Theoretically, McKee (1989) and McKee et al. (1993) point out that GMCs cannot be bound, turbulent, and magnetically subcritical. Turbulence and magnetic fields together can support a larger cloud mass than magnetic fields or turbulence alone. If the turbulent energy is comparable to the magnetic energy, as both observations and general expectations of equipartition suggest, then the critical mass arising from both sources must be $M_{\rm crit} \approx 2M_\Phi$. If the cloud is magnetically subcritical, then $M \lesssim M_\Phi$, so $M \lesssim M_{\rm crit}/2$. However, for a cloud to be bound it must be near its critical mass. A cloud that is only half its critical mass must be unbound and would certainly not be centrally concentrated. Since observations indicate that molecular clouds are both bound and centrally concentrated (see § 7.5), it follows that they must be magnetically supercritical, with $M \approx 2M_\Phi$.

Zeeman splitting observations of magnetic field strengths in Milky Way GMCs support this view. Crutcher (1999) and Bourke et al. (2001) find that $M \approx 2M_\Phi$. Galli et al. (1999) and Allen & Shu (2000) point out that this conclusion depends on the assumed cloud geometry along the line of sight and that Crutcher's data are consistent with $M \approx M_\Phi$ if clouds are highly flattened. However, this model is feasible only if true magnetic field values in regions with no detectable Zeeman splitting are near their 3 σ upper limits (Bourke et al. 2001). Furthermore, if GMCs in general are highly flattened, we ought to observe at least some of them edge-on, allowing us to see their sheetlike structure. No such sheetlike clouds have been observed. A final problem with the sheetlike cloud picture is that a highly flattened geometry is not consistent with the observation that clouds have turbulent energies comparable to their gravitational potential energies. In such a cloud, the turbulence would be strong enough to bring gas out of the cloud plane and create a more three-dimensional geometry.

Another line of observational evidence that clouds are magnetically supercritical comes from statistical indicators. Padoan et al. (2004) argue based on simulations that the magnetic fields that are at or above equipartition with the kinetic energy yield measurably different distributions of column density than fields that are below equipartition. They argue that the observations are closer to the sub-equipartition simulations. While there is some uncertainty in interpreting simulations of periodic boxes in the context of real, finite-sized molecular clouds, these simulations do provide a strong argument for magnetic supercriticality.

One final problem for magnetically mediated star formation theories is that the time required for ambipolar diffusion to change a subcritical region into one that is supercritical may be considerably shorter in turbulent media than in static media (Heitsch et al. 2004). Consequently, the long ambipolar diffusion time invoked to explain the low SFR may not apply to GMCs, which observations indicate are strongly turbulent. Li & Nakamura (2004) and Nakamura & Li (2005) perform simulations showing that in a two-dimensional geometry, turbulence does not enhance ambipolar diffusion enough to make the SFR too high, but two-dimensional turbulence and three-dimensional turbulence are very different, so it is unclear that their results in this regard are applicable to real clouds. Whether magnetic regulation with ambipolar diffusion is even capable of producing the correct star formation timescale in a turbulent medium remains an open question.

7.4. *Why Is $Q \approx 1$?*

An additional important assumption in our theory is that $Q \approx 1$. While this is well justified observationally (Quirk 1972; Kennicutt 1989; Martin & Kennicutt 2001), previous work has also provided a theoretical explanation, which is part of any complete theory of star formation. Theoretically one expects feedback effects to prevent Q from straying too far from unity. In ordinary disk galaxies like the Milky Way, supernovae are the likely feedback mechanism (Silk 1997). If Q is too low, then the SFR will increase (eq. [56]) and the supernova rate will increase as well. This will raise the temperature and the velocity dispersion in the ISM, increasing Q and reducing the SFR. If Q becomes too large compared to unity, then gravitational instability shuts off and molecular clouds cease to form. This is observed in the outer parts of disk galaxies (Kennicutt 1989). However, if there is sufficient gas present, then without continual supernova stirring the gas velocity dispersion will decrease. This will reduce Q, causing the SFR to rise again.

In starbursts, the feedback mechanism probably changes over from supernovae to radiation pressure (Thompson et al. 2005), but the effect is similar. Low Q-values raise the SFR, which increases the luminosity of the stellar population and thereby increases the radiation pressure. This puffs up the disk and restores $Q \approx 1$. If Q is much larger than unity, the SFR will fall and the disk will lose radiation pressure support and begin to collapse, reducing Q. These mechanisms complete the picture of why $Q \approx 1$.

7.5. *Are Molecular Clouds Bound?*

Our analysis also depends on molecular clouds being gravitationally bound, virialized structures. If the true virial parameter of GMCs is substantially different from unity, then $\mathrm{SFR}_{\mathrm{ff}}$ and the overall SFR will be much greater (for $\alpha_{\mathrm{vir}} \ll 1$) or smaller (for $\alpha_{\mathrm{vir}} \gg 1$) than we have estimated. Furthermore, our analysis based on the density PDF assumes that molecular clouds are gravitationally bound structures that live long enough for their density distributions to reach statistical equilibrium. If GMCs are largely unbound or consist of gas that has been compressed by shocks and that all collapses immediately (Elmegreen 2000; Hartmann et al. 2001; Clark & Bonnell 2004; Clark et al. 2005), it is not clear that the density PDF could reach its equilibrium form before the star formation process was complete. We must therefore consider whether our assumption of bound, virialized clouds is a sound one.

Observations indicate that GMC virial parameters are close to unity. McKee & Tan (2003) analyze the CO surveys of Solomon et al. (1987) and Dame et al. (1986) and find that the mean virial parameters for the large clouds in their samples, where most stars form, are 1.3 and 1.4. In M33, Rosolowsky et al. (2003) obtain velocity dispersions, masses, and radii for 36 GMCs. From their data, we find a mass-weighted mean virial parameter of 1.6. In the nucleus of M64, Rosolowsky & Blitz (2005) find that GMCs are overpressured with respect to their environments by at least a factor of 2, indicating that they too likely have $\alpha_{\mathrm{vir}} \approx 1$. Thus, our adopted value of $\alpha_{\mathrm{vir}} = 1.3$ is in good agreement with observations, both in the Milky Way and in the disks and nuclei of galaxies similar to it.

That observed virial parameters are all close to unity in itself strongly indicates that GMCs are gravitationally bound, not held together temporarily by the ram pressure of turbulent flows in the ISM. There is no reason that turbulent flows would create clouds with $\alpha_{\mathrm{vir}} \approx 1$. As an example, consider the molecular clumps inside GMCs, most of which are created by turbulent flows and confined by turbulent pressure rather than self-gravity. Most clumps have virial parameters $\alpha_{\mathrm{vir}} \gg 1$, and they have a power-law distribution of α_{vir} values for $\alpha_{\mathrm{vir}} \gtrsim 1$ (Bertoldi & McKee 1992). The same is true of molecular clouds with masses $\lesssim 10^4\ M_\odot$ (Heyer & Brunt 2004). While molecules will only form in dense regions of the ISM, and for this reason CO surveys are biased toward dense gas with low virial parameters, for the UV field of our Galaxy to be such that we see only clouds that have virial parameters of 1–2 requires an unlikely coincidence. Even if this coincidence could work in the Milky Way, it would not explain the observations in M33, where the interstellar UV flux could be quite different, and in M64, where the density of the gas prevents far-ultraviolet photons from propagating through the ISM at all.

Another strong argument that suggests that GMCs are bound is that GMCs have a characteristic mass. In the Milky Way, there is a clear upper limit on GMC masses of approximately $6\times10^6\ M_\odot$. This limit is not consistent with statistically "running out" of clouds at high masses. It is a real break in the power-law distribution that is observed at lower masses (McKee & Williams 1997). The mass distributions of GMCs in M33 (Engargiola et al. 2003) and M64 (E. Rosolowsky 2005, private communication) also exhibit characteristic scales. If GMCs are gravitationally bound, then the Jeans mass provides a natural scale that agrees reasonably well with the observations. If GMCs are not bound, however, they cannot have been created by gravitational collapse and the Jeans mass is therefore irrelevant. Turbulent flows without self-gravity are scale-free. If GMCs are unbound, they should not exhibit any characteristic mass. This prediction of the unbound GMC model is inconsistent with the observations. One cannot invoke observational selection biases to explain this inconsistency, as is done to explain the observed values of α_{vir}. Rendering the Milky Way GMC mass distribution consistent with a pure power law would require that the Milky Way contain $\approx$100 GMCs with masses larger than $6\times10^6\ M_\odot$ (McKee & Williams 1997; McKee 1999). There is no plausible way that such a large number of very massive clouds could have been missed.

7.6. *Feedback and Cloud Destruction*

Thus far we have omitted any discussion of the effects of massive star formation feedback. Obviously massive star formation gives rise to H II regions that destroy molecular clouds by photoionization and winds. Matzner (2002) estimates that this effect limits Galactic GMCs to converting at most $\sim$5%–10% of their mass into stars over their lifetimes. Our justification for neglecting this effect hinges on the difference between the star formation

efficiency, which measures the fraction of gas in a particular GMC that is transformed into stars, and the star formation *rate*, which measures the instantaneous rate at which gas is transformed into stars. Feedback from massive stars ultimately controls the star formation efficiency by disrupting a cloud before it can turn most of its mass into stars. However, feedback does not change the instantaneous SFR in the molecular gas except indirectly, by driving turbulence in the molecular gas and therefore changing the Mach number. Feedback only affects the SFR by turning molecular gas into atomic or ionized gas, thereby reducing the amount of molecular gas available to make stars. A thorough understanding of mechanisms like photoionization that regulate the amount of molecular gas available to form stars would allow us to calculate $f_{\rm GMC}$ from first principles, rather than taking it from observations, and would be an important piece of a complete theory of star formation. However, our results can stand independently of this, since $f_{\rm GMC}$ is directly observable, and our theory therefore relies only on direct observables.

7.7. *Turbulent Decay*

The largest single omission from our theory of star formation is that it does not address the critical question of what keeps GMCs in virial balance. Simulations of both hydrodynamic and magnetohydrodynamic turbulence in periodic boxes indicate that turbulence decays on timescales of a single crossing time of the object (Mac Low et al. 1998; Stone et al. 1998; Mac Low 1999; Padoan & Nordlund 1999). The crossing time is $t_{\rm cr} = 2R/\sigma$, where R is the object's radius and σ is its velocity dispersion. The crossing time and the free-fall time are related to the virial parameter by

$$\alpha_{\rm vir} = \frac{5\sigma^2 R}{GM} = \frac{40}{3\pi}\left(\frac{t_{\rm ff}}{t_{\rm cr}}\right)^2, \tag{81}$$

where M is the object's mass. In a cloud with our fiducial value of $\alpha_{\rm vir} = 1.3$, $t_{\rm cr} = 1.8t_{\rm ff}$. If the turbulence decays substantially in a single crossing time, this means that the object should enter free-fall collapse within $\sim$2 free-fall times. If that happened, then $\alpha_{\rm vir}$ would become much smaller than unity, and the majority of the gas would rapidly turn into stars. That would yield an SFR far higher than observations allow. Thus, GMCs must not be collapsing in this manner. Rapid decay of turbulence is also difficult to reconcile with several other observations (see McKee 1999 for a detailed discussion).

There are several possible explanations for the noncollapse of GMCs. First is the possibility that turbulence may not decay as quickly as the simulations indicate. Cho & Lazarian (2003) argue that Alfvén waves in a turbulent magnetized medium cascade from large to small scales and decay anisotropically, with modes along and perpendicular to the magnetic field having different decay rates. Only one mode decays as rapidly as the simulations indicate. They argue that the simulations performed to date lack the dynamic range to model this effect correctly. Similarly, Sugimoto et al. (2004) perform simulations showing that, in a filamentary cloud geometry, Alfvén waves of different polarizations decay at different rates, with some modes decaying twice as slowly as earlier simulations indicated. If these results from somewhat idealized cases apply to real clouds, then GMCs could live for several free-fall times, long enough to allow the formation of massive stars that could disrupt them rather than letting them collapse entirely into stars.

A second possibility is that turbulence in GMCs is driven by continual perturbations from outside that are strong enough to prevent the decay of turbulence and keep GMCs virialized. Kornreich & Scalo (2000) suggest that GMCs will be struck by supernova shock waves that maintain cloud turbulence at intervals comparable to the free-fall times of large GMCs. However, this source of driving is highly stochastic, so it is unclear that the shocks can truly keep most clouds from collapsing. Furthermore, F. Nakamura et al. (2005, in preparation) perform numerical studies indicating that it may not be possible for external shocks to drive turbulence in clouds without disrupting them entirely. Koyama & Inutsuka (2002) suggest that turbulence is driven by thermal instability at the interface between atomic and molecular gas. However, the characteristic size scale of the disturbances this creates is only $\sim$0.1 pc, so it is unclear that this turbulence would be able to affect the interiors of GMCs. Piontek & Ostriker (2004) consider thermal plus magnetorotational instability in the atomic phase of the ISM and find that magnetic fields allow motions generated at the warm-cold interface to drive turbulence far from the interface. However, it is unknown if this mechanism would work in GMCs. Furthermore, thermal instability offers no clear way to explain turbulence in GMCs in galaxies like M64 where the ISM has no atomic phase and is not known to be thermally bistable as is the atomic ISM in the Milky Way.

A third possible solution to the problem of turbulent decay is driving by feedback from star formation. Norman & Silk (1980) and McKee (1989) argue based on analytic calculations that, for the observed SFR, the rate at which protostellar outflows inject energy into their parent clouds is sufficient to balance the rate at which turbulence decays. Quillen et al. (2005) observe protostellar outflow cavities in NGC 1333 and estimate that the rate of energy injection from the observed cavities is sufficient to power the turbulence of the cloud, in agreement with this model. Matzner (2002) argues that when massive stars are present, turbulent motions driven by the overpressure in H II regions are the dominant source of energy injection. Matzner estimates analytically that the energy injection rate by H II regions is sufficient to balance the turbulent decay rate even if the decay time is only a crossing time. However, the theory depends on an efficiency of energy injection by H II regions that has only been estimated analytically and ideally should be set by simulations.

Regardless of the true mechanism, the observations show that GMCs cannot be collapsing completely and rapidly. The exact mechanism by which the turbulence is maintained does not affect our analysis because, below the scale at which it is driven, all turbulence is the same. That is why, for example, simulations find a universal density PDF independent of whether the turbulence is driven or undriven and regardless of the random realization of the initial velocity field or driving field. Observed GMCs in both the Milky Way and other galaxies are virialized, with turbulence balancing gravity, and we have shown here that virialized, turbulent clouds produce an SFR that is consistent with observations. The remaining significant piece of this theory, which we leave for future work, is an explanation for how the observed virial balance is maintained.

8. CONCLUSIONS

In this work we have attempted to fill in a significant missing piece of the overall picture of star formation: a quantitative theory that can map the conditions in a star-forming region into an SFR based on simple physical principles. Our basic picture is that stars form in gravitationally bound, virialized molecular clouds. Only 1%–2% of a cloud is transformed into stars in a single free-fall time because in a turbulent virialized cloud, most of the gas is in structures that have more kinetic energy

than gravitational potential energy. Only rare, overdense regions are gravitationally bound, and the fraction of a cloud's mass in such regions is nearly a constant $\sim$1% over all virialized clouds. We have for the first time computed the collapsing mass fraction directly in terms of the Mach number and the virial parameter, the two basic dimensionless numbers that describe a star-forming cloud, and shown that the fraction of gas in collapsing structures is only a very weak function of the Mach number for virialized clouds. The SFR is simply the mass in sufficiently overdense structures divided by the cloud free-fall time. Our model does not rely on an unknown efficiency of star formation or an unknown critical density. The only inputs are the physics of turbulence and the virial theorem.

This prescription correctly predicts the SFR when we apply it to the observed giant molecular clouds in the Milky Way. We also estimate the properties of star-forming clouds in other galaxies as a function of the rotation speeds and surface densities of various components in those galaxies. We use these estimated cloud properties combined with our prediction for the SFR in a cloud to compute galactic-average SFRs and show that our predictions agree with the observed SFR in a sample of galaxies ranging from normal disks like the Milky Way to starbursts and ULIRGs. Thus, our theory provides a unified model capable of explaining the star formation on scales from the individual clouds within a galaxy to the entire star-forming disk of a starburst or normal disk galaxy.

The authors thank Leo Blitz, Norm Murray, Eliot Quataert, Eric Rosolowsky, Jonathan Tan, and Todd Thompson for helpful discussions. C. F. M. acknowledges the support of NSF grant AST 00-98365.

APPENDIX A

ESTIMATING ϕ_P

We estimate ϕ_P by considering cases ranging from normal disks to starbursts. In the solar neighborhood, the total disk surface density is $\Sigma_{\rm tot} \approx 56\,M_\odot\,{\rm pc}^{-2}$ (Holmberg & Flynn 2004), and the gas surface density is $\Sigma_g \approx 12\,M_\odot\,{\rm pc}^{-2}$ (Boulares & Cox 1990), so $f_g \approx 0.21$. The total midplane pressure is $P \approx 3.9\times10^{-12}$ dyn cm^{-2}, but approximately 1.9×10^{-12} dyn cm^{-2} of this comes from magnetic fields and cosmic rays (Boulares & Cox 1990). Since these permeate the molecular clouds and the nonmolecular gas equally, they provide no confining pressure on molecular clouds. The effective pressure on GMCs in the Milky Way, therefore, is roughly 2×10^{-12} dyn cm^{-2}. For the Milky Way solar neighborhood values of $\Sigma_{\rm tot}$ and Σ_g, we find $\phi_{\rm mp} = 0.50$. Thus, $\phi_P \approx 2.4$ in the solar neighborhood.

At the opposite extreme consider a starburst or ULIRG. Downes & Solomon (1998) find that the gas fraction in high surface density starbursts is $f_g \approx \frac{1}{3}$. We cannot directly observe $\phi_{\rm mp}$ in starbursts, but we can estimate it based on physical considerations. The reason $\phi_{\rm mp} < 1$ in the Milky Way is that the gas scale height is small compared to the stellar scale height. This occurs because the gas comprises a small fraction of the total surface density of the disk and because old stars have had a long time to scatter off molecular clouds (Rafikov 2001). In a starburst, the gas fraction is considerably higher and there is no population of old stars that have had a long time to be dynamically heated (Downes & Solomon 1998). We therefore expect that stars and gas will have comparable scale heights, which will produce $\phi_{\rm mp} \approx 1$. This gives $\phi_P = 3$ in starbursts.

Since ϕ_P seems roughly constant over a range of environments from the solar neighborhood to extreme starbursts, we adopt a constant value of $\phi_P = 3$ throughout our work. The plausible range of variation of ϕ_P is from $\sim$1, corresponding to a purely gaseous disk, to $\sim$6, corresponding to a starburst containing only $\frac{1}{6}$ gas, the rough lower limit in the Downes & Solomon (1998) sample.

Note that because GMCs occupy a relatively small fraction of the ISM, one might treat them as a pressureless component like stars rather than a pressure-contributing component like atomic gas. This would reduce ϕ_P. However, since within a GMC the molecular gas does contribute pressure, the product $\phi_P\phi_{\overline{P}}$ must remain unchanged. Thus, if one takes a smaller value for ϕ_P, one must use a correspondingly larger value for $\phi_{\overline{P}}$. Since our predicted SFR depends on $\phi_P\phi_{\overline{P}}$, there would be no net change to our predictions.

APPENDIX B

ESTIMATING $\phi_{\overline{P}}$

In an environment where the ISM is predominantly atomic, such as the Milky Way, interstellar UV photons dissociate H_2 and CO that is not sufficiently shielded. Thus, molecular clouds exist only as the inner parts of atomic-molecular complexes (Elmegreen 1989, 1994). Since atomic and molecular hydrogen cannot cool effectively, star formation only occurs in the parts of the complexes where CO is present. For Milky Way interstellar UV fluxes, a layer of gas where C is atomic must provide at least $\sim$0.7 mag of extinction to prevent dissociation of CO (van Dishoeck & Black 1988). With such a shielding layer, the mean pressure in the molecular gas is higher than in the combined atomic and molecular complex. Holliman (1995) estimates $\phi_{\overline{P}} \approx 8$, which is consistent with the observed ratios of GMC pressure to ISM pressure in the Milky Way (Blitz 1993). However, there is considerable uncertainty in applying this estimate to other galaxies because it depends on the metallicity of the galactic ISM and the strength of the interstellar UV field, both of which vary considerably from galaxy to galaxy.

For galaxies where the ISM is purely molecular, clouds are not exposed to any external UV flux. In this case, we assume that clouds can be described very roughly as polytropic spheres. For a polytropic cloud with $P \propto r^{-k_P}$,

$$\phi_{\overline{P}} = \frac{3}{3 - k_P}. \tag{B1}$$

For an isothermal sphere, $k_P = 2$ so $\phi_{\overline{P}} = 3$. For a cloud with a density profile $\rho \propto r^{-1}$, $\phi_{\overline{P}} = 1$. We consider these extreme limits and take $\phi_{\overline{P}} = 2$ as a typical value. This is consistent with observations of GMCs in purely molecular galaxies (Rosolowsky & Blitz 2005).

We adopt a very rough formula to interpolate between the purely atomic and purely molecular cases:

$$\phi_{\overline{P}} = 10 - 8 f_{\rm GMC}, \tag{B2}$$

where $f_{\rm GMC} \equiv \Sigma_{\rm mol}/\Sigma_g$ is the molecular gas fraction. One could also have chosen to use a step function approximation or simply taken $\phi_{\overline{P}} = 6$ as a universal value covering the range from starbursts to ordinary disks. We consider any value of $\phi_{\overline{P}}$ from 2 to 10 reasonable, although a value of 2 is implausible for a galaxy with a great deal of atomic gas, and a value of 10 is implausible for a galaxy that is entirely molecular.

REFERENCES

Allen, A., & Shu, F. H. 2000, ApJ, 536, 368
Balbus, S. A. 1988, ApJ, 324, 60
Bate, M. R., Bonnell, I. A., & Price, N. M. 1995, MNRAS, 277, 362
Bertoldi, F., & McKee, C. F. 1992, ApJ, 395, 140
Binney, J., & Merrifield, M. 1998, Galactic Astronomy (Princeton: Princeton Univ. Press)
Blitz, L. 1993, in Protostars and Planets III, ed. E. H. Levy & J. I. Lunine (Tucson: Univ. Arizona Press), 125
Blitz, L., & Rosolowsky, E. 2004, ApJ, 612, L29
Bonnor, W. B. 1956, MNRAS, 116, 351
Boulares, A., & Cox, D. P. 1990, ApJ, 365, 544
Bourke, T. L., Myers, P. C., Robinson, G., & Hyland, A. R. 2001, ApJ, 554, 916
Bronfman, L., Casassus, S., May, J., & Nyman, L.-Å. 2000, A&A, 358, 521
Cho, J., & Lazarian, A. 2003, MNRAS, 345, 325
Clark, P. C., & Bonnell, I. A. 2004, MNRAS, 347, L36
Clark, P. C., Bonnell, I. A., Zinnecker, H., & Bate, M. R. 2005, MNRAS, 359, 809
Crutcher, R. M. 1999, ApJ, 520, 706
Dame, T. M., Elmegreen, B. G., Cohen, R. S., & Thaddeus, P. 1986, ApJ, 305, 892
Dame, T. M., et al. 1987, ApJ, 322, 706
Downes, D., & Solomon, P. M. 1998, ApJ, 507, 615
Ebert, R. 1955, Z. Astrophys., 37, 217
Elmegreen, B. G. 1989, ApJ, 338, 178
———. 1994, ApJ, 433, 39
———. 2000, ApJ, 530, 277
———. 2002, ApJ, 577, 206
———. 2003, Ap&SS, 284, 819
Elmegreen, B. G., & Scalo, J. 2004, ARA&A, 42, 211
Engargiola, G., Plambeck, R. L, Rosolowsky, E., & Blitz, L. 2003, ApJS, 149, 343
Fukui, Y., Norikazu, M., Yamaguchi, R., Mizuno, A., & Toshikazu, O. 2001, PASJ, 53, L41
Galli, D., Lizano, S., Li, Z.-Y., Adams, F. C., & Shu, F. H. 1999, ApJ, 521, 630
Gao, Y., & Solomon, P. M. 2004, ApJ, 606, 271
Genzel, R., Tacconi, L. J., Rigopoulou, D., Lutz, D., & Tecza, M. 2001, ApJ, 563, 527
Hartmann, L., Ballesteros-Pardes, J., & Bergin, E. A. 2001, ApJ, 562, 852
Heckman, T. M., Lehnert, M. D., Strickland, D. K., & Armus, L. 2000, ApJS, 129, 493
Heiles, C., & Troland, T. H. 2003, ApJ, 586, 1067
Heitsch, F., Zweibel, E. G., Slyz, A. D., & Devriendt, J. E. G. 2004, ApJ, 603, 165
Heyer, M. H., & Brunt, C. M. 2004, ApJ, 615, L45
Heyer, M. H., Carpenter, J. M., & Snell, R. L. 2001, ApJ, 551, 852
Holliman, J. H. 1995, Ph.D. thesis, Univ. California, Berkeley
Holmberg, J., & Flynn, C. 2004, MNRAS, 352, 440
Jog, C. J., & Solomon, P. M. 1984, ApJ, 276, 114
Johnstone, D., Di Francesco, J., & Kirk, H. 2004, ApJ, 611, L45
Kennicutt, R. C., Jr. 1989, ApJ, 344, 685
———. 1998a, ApJ, 498, 541
———. 1998b, ARA&A, 36, 189
Kim, W.-T., & Ostriker, E. C. 2001, ApJ, 559, 70
Kim, W.-T., Ostriker, E. C., & Stone, J. M. 2002, ApJ, 581, 1080
———. 2003, ApJ, 599, 1157
Klessen, R. S., Heitsch, F., & Mac Low, M.-M. 2000, ApJ, 535, 887
Kornreich, P., & Scalo, J. 2000, ApJ, 531, 366
Koyama, H., & Inutsuka, S.-I. 2002, ApJ, 564, L97
Kravtsov, A. V. 2003, ApJ, 590, L1
Krumholz, M. R., McKee, C. F., & Klein, R. I. 2004, ApJ, 611, 399
Larson, R. B. 1981, MNRAS, 194, 809
Li, P. S., Norman, M. L., Mac Low, M.-M., & Heitsch, F. 2004, ApJ, 605, 800
Li, W., Evans, N. J., II, & Lada, E. A. 1997, ApJ, 488, 277
Li, Y., Mac Low, M.-M., & Klessen, R. S. 2005, ApJ, 620, L19
Li, Z.-Y., & Nakamura, F. 2004, ApJ, 609, L83
Mac Low, M.-M. 1999, ApJ, 524, 169
Mac Low, M.-M., & Klessen, R. S. 2004, Rev. Mod. Phys., 76, 125
Mac Low, M.-M., Klessen, R. S., Burkert, A., & Smith, M. D. 1998, Phys. Rev. Lett., 80, 2754
Martin, C. L., & Kennicutt, R. C., Jr. 2001, ApJ, 555, 301
Matzner, C. D. 2002, ApJ, 566, 302
Matzner, C. D., & McKee, C. F. 2000, ApJ, 545, 364
McKee, C. F. 1989, ApJ, 345, 782
———. 1999, in The Origin of Stars and Planetary Systems, ed. C. J. Lada & N. D. Kylafis (Dordrecht: Kluwer), 29
McKee, C. F., & Holliman, J. H., II 1999, ApJ, 522, 313
McKee, C. F., & Tan, J. C. 2003, ApJ, 585, 850
McKee, C. F., & Williams, J. P. 1997, ApJ, 476, 144
McKee, C. F., Zweibel, E. G., Goodman, A. A., & Heiles, C. 1993, in Protostars and Planets III, ed. E. H. Levy & J. I. Lunine (Tucson: Univ. Arizona Press), 327
Mouschovias, T. Ch. 1987, in Physical Processes in Interstellar Clouds, ed. G. E. Morfill & M. Scholer (NATO ASI Ser. C, 210; Dordrecht: Reidel), 453
Nakamura, F., & Li, Z.-Y. 2005, ApJ, submitted (astro-ph/0502130)
Nakanishi, H., & Sofue, Y. 2003, PASJ, 55, 191
Navarro, J. F., Frenk, C. S., & White, S. D. M. 1997, ApJ, 490, 493
Navarro, J. F., et al. 2004, MNRAS, 349, 1039
Nordlund, Å., & Padoan, P. 1999, in Interstellar Turbulence, ed. J. Franco & A. Carramiñana (Cambridge: Cambridge Univ. Press), 218
Norman, C., & Silk, J. 1980, ApJ, 238, 158
Ossenkopf, V., & Mac Low, M.-M. 2002, A&A, 390, 307
Ostriker, E. C., Gammie, C. F., & Stone, J. M. 1999, ApJ, 513, 259
Padoan, P. 1995, MNRAS, 277, 377
Padoan, P., Jimenez, R., Juvela, M., & Nordlund, Å. 2004, ApJ, 604, L49
Padoan, P., & Nordlund, Å. 1999, ApJ, 526, 279
———. 2002, ApJ, 576, 870
———. 2004, ApJ, 617, 559
Padoan, P., Nordlund, Å., & Jones, B. 1997, MNRAS, 288, 145
Passot, T., & Vázquez-Semadeni, E. 1998, Phys. Rev. E, 58, 4501
Piontek, R. A., & Ostriker, E. C. 2004, ApJ, 601, 905
Plume, R., Jaffe, D. T., Evans, N. J., II, Martín-Pintado, J., & Gómez-González, J. 1997, ApJ, 476, 730
Quillen, A. C., Thorndike, S. L., Cunningham, A., Frank, A., Gutermuth, R. A., Blackman, E. G., Pipher, J. L., & Ridge, N. 2005, ApJ, submitted (astro-ph/0503167)
Quirk, W. J. 1972, ApJ, 176, L9
Rafikov, R. R. 2001, MNRAS, 323, 445
Rosolowsky, E., & Blitz, L. 2005, ApJ, 623, 826
Rosolowsky, E., Engargiola, G., Plambeck, R., & Blitz, L. 2003, ApJ, 599, 258
Rownd, B. K., & Young, J. S. 1999, AJ, 118, 670
Scalo, J. M., Vázquez-Semadeni, E., Chappell, D., & Passot, T. 1998, ApJ, 504, 835
Schmidt, M. 1959, ApJ, 129, 243
———. 1963, ApJ, 137, 758
Seljak, U. 2002, MNRAS, 334, 797
Shu, F. H., Adams, F. C., & Lizano, S. 1987, ARA&A, 25, 23
Silk, J. 1997, ApJ, 481, 703
Soifer, B. T., et al. 2000, AJ, 119, 509
Solomon, P. M., Downes, D., Radford, S. J. E., & Barrett, J. W. 1997, ApJ, 478, 144
Solomon, P. M., Rivolo, A. R., Barrett, J., & Yahil, A. 1987, ApJ, 319, 730
Stone, J. M., Ostriker, E. C., & Gammie, C. F. 1998, ApJ, 508, L99
Sugimoto, S., Hanawa, T., & Fukuda, N. 2004, ApJ, 609, 810
Tan, J. C. 2000, ApJ, 536, 173
Tassis, K., & Mouschovias, T. Ch. 2004, ApJ, 616, 283
Thompson, T. A., Quataert, E., & Murray, N. 2005, ApJ, 630, 167
Toomre, A. 1964, ApJ, 139, 1217
Tully, R. B., & Fisher, J. R. 1977, A&A, 54, 661
van Dishoeck, E. F., & Black, J. H. 1988, ApJ, 334, 771
Vázquez-Semadeni, E. 1994, ApJ, 423, 681
Vázquez-Semadeni, E., Ballesteros-Paredes, J., & Klessen, R. S. 2003, ApJ, 585, L131 (VBK03)

Vázquez-Semadeni, E., Kim, J., Shadmehr, M., & Ballesteros-Paredes, J. 2005, ApJ, 618, 344
Williams, J. P., & McKee, C. F. 1997, ApJ, 476, 166
Wolfire, M. G., McKee, C. F., Hollenbach, D., & Tielens, A. G. G. M. 2003, ApJ, 587, 278
Wong, T., & Blitz, L. 2002, ApJ, 569, 157
Young, J. S., Allen, L., Kenney, J. D. P., Lesser, A., & Rownd, B. 1996, AJ, 112, 1903
Zuckerman, B., & Evans, N. J., II 1974, ApJ, 192, L149